

# THE MECHANICAL PROPERTIES OF HUMAN DENTIN: A CRITICAL REVIEW AND RE-EVALUATION OF THE DENTAL LITERATURE

---

J.H. Kinney\*  
S.J. Marshall  
G.W. Marshall

Division of Biomaterials and Bioengineering, Department of Preventive and Restorative Dental Sciences, Mail Stop 0758, University of California, San Francisco, San Francisco, CA 94143-0758;  
\*corresponding author, kinney3@llnl.gov

**ABSTRACT:** The past 50 years of research on the mechanical properties of human dentin are reviewed. Since the body of work in this field is highly inconsistent, it was often necessary to re-analyze prior studies, when possible, and to re-assess them within the framework of composite mechanics and dentin structure. A critical re-evaluation of the literature indicates that the magnitudes of the elastic constants of dentin must be revised considerably upward. The Young's and shear moduli lie between 20-25 GPa and 7-10 GPa, respectively. Viscoelastic behavior (time-dependent stress relaxation) measurably reduces these values at strain rates of physiological relevance; the reduced modulus (infinite relaxation time) is about 12 GPa. Furthermore, it appears as if the elastic properties are anisotropic (not the same in all directions); sonic methods detect hexagonal anisotropy, although its magnitude appears to be small. Strength data are re-interpreted within the framework of the Weibull distribution function. The large coefficients of variation cited in all strength studies can then be understood in terms of a distribution of flaws within the dentin specimens. The apparent size-effect in the tensile and shear strength data has its origins in this flaw distribution, and can be quantified by the Weibull analysis. Finally, the relatively few fracture mechanics and fatigue studies are discussed. Dentin has a fatigue limit. For stresses smaller than the normal stresses of mastication, ~ 30 MPa, a flaw-free dentin specimen apparently will not fail. However, a more conservative approach based on fatigue crack growth rates indicates that if there is a pre-existing flaw of sufficient size (~ 0.3-1.0 mm), it can grow to catastrophic proportion with cyclic loading at stresses below 30 MPa.

**Key words.** Dentin, calcified tissues, mechanical properties, fatigue, fracture toughness.

## Introduction

Dentin is the most abundant mineralized tissue in the human tooth. Therefore, knowledge of its mechanical properties is essential for predicting the effects of microstructural alterations due to caries, sclerosis, and aging on tooth strength. In clinical dentistry, knowledge of dentin properties is important for understanding the effects of the wide variety of restorative dental procedures that range from the design of preparations to choice of bonding methods.

In spite of this importance, over half a century of research has failed to provide consistent values of dentin's mechanical properties. The Young's modulus is unknown to within a factor of three; the shear modulus is uncertain by a factor of four; and the other elastic constants have not been measured. There is a six-fold uncertainty in the ultimate strength, and there have been few studies of fracture toughness or fatigue.

This is a review of the last 50+ years of research into the mechanical properties of dentin. It is a critical review, in the sense that the prior literature on the mechanical properties of dentin is often re-examined and re-interpreted within the context of dentin microstructure. For example, the widely varying tensile strength data are re-examined in terms of the Weibull distribution function; the wide variations in previously reported tensile strengths can then be explained by a specimen size effect whose origin lies in the existence of a population of flaws in the dentin.

The bulk of this review focuses on the elastic properties of dentin. This emphasis is a necessary consequence of both the paucity of published data on other mechanical properties, and the fact that an understanding of elastic behavior is essential to the proper interpretation of physical measurements of failure. It was often necessary to re-evaluate the data on the elastic properties to reconcile the contradictions in the literature and reach consensus. Because the physical data were frequently not available in the more recent publications, indirect methods were used to test the meaningfulness of the results. This involved consideration of the entire elastic stiffness matrix to check the constraints forced upon all of the elastic constants from the measurement of a single property. In this way, it was possible to check for self-consistency with all of the elastic constants as well as the known microstructure.

After a brief discussion of the composition and microstructure of dentin, the review first considers its elastic and viscoelastic properties. Then, hardness, strength, fracture toughness, and fatigue are discussed in order. This organization loosely follows that of the last comprehensive review of dentin properties (Waters, 1980), with the exception that a more thorough treatment of fatigue and fracture toughness has been added. The review concludes by proposing reliable ranges for the magnitudes of mechanical properties. It is hoped that these recommendations, and the evidence on which they are based, spark additional discourse and research on the properties of dentin.

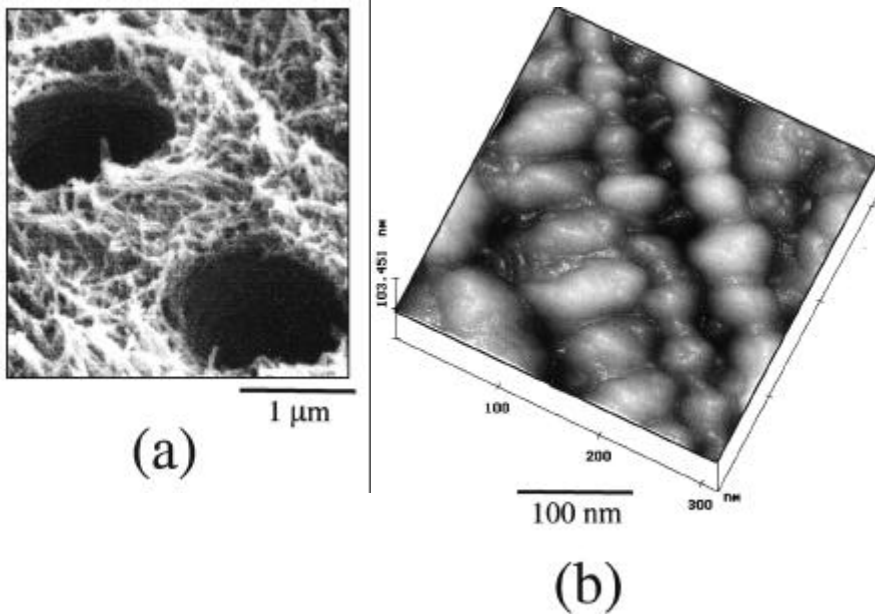


**Figure 1.** (a) SEM image of a fixed, demineralized dentin specimen showing the collagen fibrils that are randomly oriented in the plane perpendicular to the tubule lumens (after Marshall *et al.*, 1997). (b) A higher-resolution AFM image of an unfixed specimen obtained in water. The AFM image shows the periodic 67-nm hole and overlap zones characteristic of the Type I collagen fibrils found in dentin and bone (after Marshall *et al.*, 2001; Habelitz *et al.*, 2002b).

## Dentin Microstructure

The microstructure of dentin suggests a hierarchical approach to the understanding of its mechanical properties. At the smallest length scales are the constituent materials: a carbonated nanocrystalline apatite mineral phase (approximately 50% by volume) and a felt-work of type I collagen fibrils (see Fig. 1). The collagen fibrils, approximately 30% by volume, are roughly 50-100 nm in diameter; they are randomly oriented in a plane perpendicular to the direction of dentin formation (Jones and Boyde, 1984). The mineral occupies two sites within this collagen scaffold: intrafibrillar (inside the periodically spaced gap zones in the collagen fibril) and extrafibrillar (in the interstices between the fibrils). The partitioning between these two sites is uncertain, although it is believed that between 70 and 75% of the mineral may be extrafibrillar (Bonar *et al.*, 1985; Pidaparti *et al.*, 1996). The mineral crystallites are needle-like near the pulp; the shape continuously progresses to plate-like with proximity to the enamel (Kinney *et al.*, 2001b). The crystallite thickness, ~ 5 nm, is invariant with location.

At a higher level of organization is an intermediate, or composite, length scale. At this length scale, dentin can be modeled as a continuous fiber-reinforced composite, with the intertubular dentin forming the matrix and the tubule lumens with their associated cuffs of peritubular dentin forming the cylindrical fiber reinforcement (see Fig. 2). The tubules run continuously from the dentin-enamel junction to the pulp in coronal dentin, and from the cementum-dentin junction to the pulp canal in the root. The regular, almost uni-axial, alignment of the tubules has led some to suggest that they play an important function in the orientation dependence of the mechanical properties (Waters, 1980).

At the greatest length scale are the effective, or continuum, properties of dentin. The effective properties of dentin describe the response of the tooth to applied loads, and allow for predictions of tooth strength and fracture properties. Young's modulus, tensile and compressive strength, and fracture toughness are examples of these effective properties, and reflect the complex interactions of the constituent materials and the microstructure. At this largest length scale, we anticipate that the effective properties will depend on tubule density, orientation, and the local average density of the mineral phase. Ultimately, measurement of the effective properties, particularly the properties of altered forms of dentin (such as carious or transparent), will benefit from an understanding of the material behavior at all of these length scales.

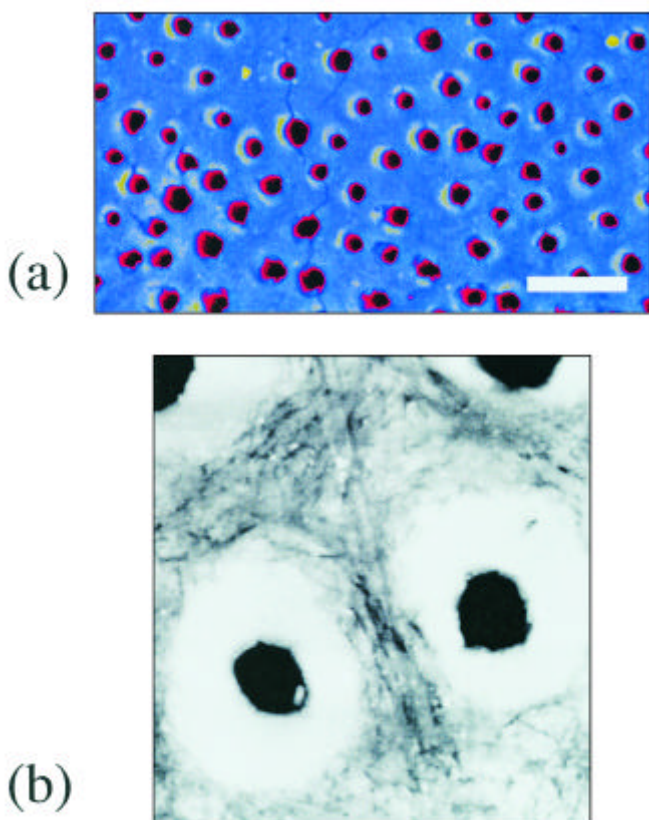


**Figure 2.** (a) SEM and (b) AFM images of fully mineralized dentin specimens showing the tubule lumens with surrounding cuffs of peritubular dentin. The bar in the SEM photomicrograph is 10 μm. Labeling: L = tubule lumen, PT = peritubular dentin, IT = intertubular dentin matrix. SEM image after Kinney *et al.* (2001a). AFM image after Kinney *et al.* (1993).

## The Elastic Properties of Dentin

The elastic properties of dentin are of paramount importance in all discussions of tooth strength. The elastic constants, usually defined in terms of a stiffness ( $C_{ij}$ ) or compliance ( $S_{ij}$ ) matrix, include the Young's modulus, shear modulus, and Poisson's ratio. Depending on the symmetry of the microstructure, the elastic constants have different degrees of independence. For example, an isotropic structure has only two independent elastic constants, while an orthotropic structure has nine independent elastic constants. Therefore, any study of the elastic properties of dentin must consider its symmetry.

## THE YOUNG'S MODULUS

The slope of the proportional part of the stress-strain curve provides the Young's modulus, while the yield strength and the ultimate strength can be obtained from the nonlinear region of the stress-strain curve. Because uni-axial stress-strain behavior is among the most straightforward of measurements, it is surprising that there is so much uncertainty in the value of Young's modulus for dentin obtained by this method. This uncertainty in Young's modulus extends to all measurement techniques, including bending, indentation, and ultrasound. A graphed representation of the measurements of Young's modulus with the year in which they were reported is shown in Fig. 3. The mean and standard deviation of these values are 13.2 GPa and 4.0 GPa, respectively. Unfortunately, over the past 50 years there has been an increase in the dispersion of the reported values; there is no evidence that this trend is abating. Therefore, it is appropriate to begin discussion of the Young's modulus of dentin by considering the constituent and composite-level organizational hierarchies in the hope that they may aid readers in discriminating between valid and invalid determinations of the effective modulus.

### Constituent materials models

An early attempt to provide reasonable bounds for the continuum Young's modulus of dentin was proposed by Katz (1971). Dentin was considered to be a two-phase mixture of apatite mineral and collagen, with the volume fraction and Young's modulus of the mineral phase given by  $V_A$  and  $E_A$ , respectively, and the corresponding values for the collagen given by  $V_C$  and  $E_C$ . The effective Young's modulus of the mixture ( $E_e$ ) was rigorously bounded from above and below by:

$$E_e \leq V_A E_A + V_C E_C \equiv V_A (E_A - E_C) + E_C \quad (1)$$

$$E_e \geq \frac{E_A E_C}{V_A E_C + V_C E_M} \quad (2)$$

The elastic properties of the constituent materials in their bulk form have been measured with reasonable accuracy:  $E_A \sim 110$  GPa and  $E_C < 0.001$  GPa (Katz and Ukraincik, 1971; Balooch *et al.*, 1998). Substitution of these values into the above equations generates the upper and lower bounds for the Young's modulus that are shown in Fig. 4. Unfortunately, the large disparity between the moduli of the two phases leads to a wide separation between the upper and lower bounds in the vicinity of the known mineral concentration in dentin (40-50% by volume). The separation between the bounds is narrowed only slightly by the application of more restrictive, variational bounding methods (Hashin, 1983). Clearly, bounds based on the constituent materials properties are of no use for discriminating between experimental measurements, all of which lie well within the upper and lower bounds predicted in Eqs. 1 and 2.

**Figure 4.** The upper (dashed line) and lower (solid line) theoretical bounds for the Young's modulus of a composite of hydroxyapatite mineral and type I collagen fibrils as calculated from Eqs. 1 and 2. The experimental data are shown as the solid bar at a volume percent mineral phase (45%) corresponding to the known composition of dentin. The graph emphasizes the difficulties of modeling mineralized tissues with bounds; The large difference in moduli between the two phases separates the upper and lower bounds by too great a magnitude to be useful.

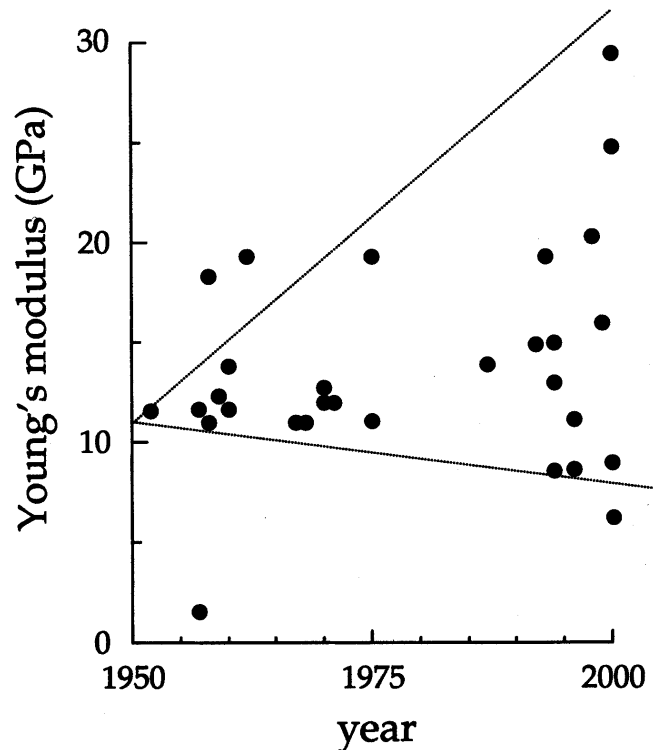
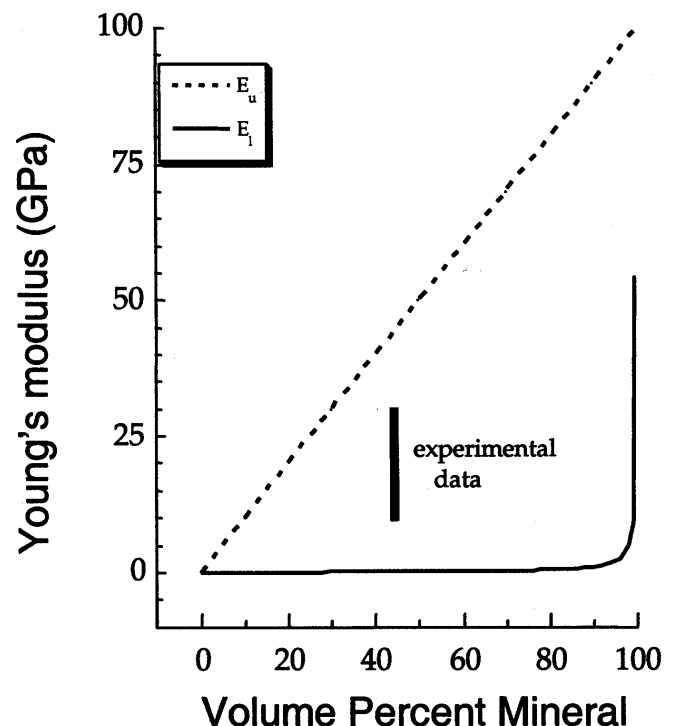


**Figure 3.** The Young's modulus as reported in the literature over the past 50 years. The data prior to 1999 appear in tabular form in the reference by Kinney *et al.* (1999). Data after 1999 are from Huo *et al.* (2000), Kinney *et al.* (2001a), Kishen *et al.* (2000), and Palamara *et al.* (2000). In the past few years, there has been a four-fold variation in the reported magnitude of the Young's modulus; the uncertainty in its value appears to be expanding with time. The uncertainty in the magnitude of the Young's modulus is probably not reflective of the actual variations in the mechanical properties of dentin. Rather, the uncertainty most likely arises from either a viscoelastic response (stress relaxation) or experimental artifact.



## Micromechanics models

Because of the large difference in modulus between the mineral and organic phases, we do not anticipate that improvement can be made by further refinements of bounds. Therefore, it is worthwhile considering a micromechanics approach at the composite hierarchy of dentin microstructure. At this length scale, the dentinal tubules with their surrounding peritubular cuffs are like fibers, providing reinforcement to the intertubular matrix. Assuming that the moduli of the matrix ( $E_M$ ) and the "fibers" (the lumens plus peritubular cuffs,  $E_F$ ) are known, rough estimates of the bounds can be made by appropriate substitutions into Eqs. 1 and 2. However, direct substitution of  $E_M$  and  $E_F$  ignores the possibly complex interactions between the "fibers" and the matrix.

The interactions between fiber and matrix have been accounted for in self-consistent generalized micromechanics approaches to aligned fiber composites (Christensen, 1990). Analytical solutions have been derived for the case of aligned cylindrical fibers in an isotropic matrix. The fibers introduce a transverse anisotropy and require five equations for the independent elastic constants to be defined. These equations have been reformulated for dentin in terms of the Young's modulus of intertubular ( $E_I$ ) and peritubular ( $E_{pt}$ ) dentin (Kinney *et al.*, 1999). The expression for the effective longitudinal (in the direction of the tubules) Young's modulus,  $E_{el}$ , in terms of the tubule concentration,  $c$ , was derived:

$$E_{el} = cE_{pt} \left( 1 - \frac{A_I}{A_{pt} + A_I} \right) + (1 - c)E_I + \gamma(c, \nu_I, \nu_{pt}) \quad (3)$$

In the above equation,  $\gamma$  is a "clamping" factor that accounts for mismatch in Poisson's ratio between the peritubular and intertubular dentins, and  $A_I$  and  $A_{pt}$  are the area fractions of the intertubular and peritubular dentin, respectively. The area ratio in Eq. 3 is apparently constant with position in the tooth, and is approximately equal to 0.25 (Pashley, 1989).

Only when the ratio of the peritubular and intertubular dentin moduli is greater than 3 is there a measurable effect of the tubules on stiffness for physiologically relevant tubule densities (5-15%). Thus, a theoretical framework now exists for estimating the effects of tubule orientation on the elastic properties: For physiologically relevant tubule densities, the anisotropy caused by the tubules is insignificant (Kinney *et al.*, 1999). This does not mean that dentin is elastically isotropic; rather, if dentin proves to be anisotropic, it is because the intertubular dentin matrix is anisotropic and not because of the tubules. Based on observations that the collagen fibrils in the intertubular matrix are aligned perpendicular to the tubule axis, we anticipate that dentin might have a transverse isotropic (hexagonal) symmetry (stiffer in the plane of the collagen fibrils).

The micromechanics model offers several advantages over bounding methods. Key is the ability of the model to make accurate estimates of the effective elastic constants based on a few simple measurements of the tubule concentration. The model has its drawbacks, however. Accurate values of the elastic constants of peritubular and intertubular dentin must be available, and this requires careful mechanical testing, which we will now review in greater detail.

## Tensile and compressive measurements of Young's modulus

There have been numerous experimental attempts to measure the Young's modulus of dentin. The majority of these measurements have been performed in either tension or compression. The primary emphasis of the tensile studies was to establish the ultimate tensile strength (UTS) of dentin; the determination of the Young's modulus appeared to be secondary to this effort.

The earliest "modern" measurement of Young's modulus in tension was published in 1962 (Bowen and Rodriguez, 1962). In that study, specimens of dentin, nominally 2 mm thick, were cut freehand with a rotary diamond disk under constant water irrigation. The specimens were narrowed in the middle, with a "radiused" shoulder (fillet) maintained so that stress concentration would be prevented. The knife-edges of an optical strain gauge (length, 6 mm) were attached directly to the specimens. The specimens were hydrated at least 1 hr in distilled water before being tested. The stress-strain curves were linear to failure, and the mean modulus of elasticity was 19.3 GPa ( $2.8 \times 10^6$  psi) with a coefficient of variation of 28%.

Five years later, Lehman (1967) measured the tensile properties of dentin with hollowed, cylindrical specimens from the root. As in the earlier study by Bowen and Rodriguez, the tensile stress-strain curves were linear to failure. However, the Young's modulus was 11.0 GPa, almost half that of the earlier study, and the coefficient of variation (53%) was almost double.

There were three important differences between the two studies. First, the latter study did not use strain gauges affixed to the specimen, thereby increasing the likelihood of grip effects like tow-in. Second, the specimens were hollowed along the root canal by means of a dental bur, increasing the probability of undetected flaws in the interior of the specimen. Third, the gauge sections were not "radiused", leaving a stress concentration that increased the chance of failure at grip ends, thereby invalidating the test.

Though it is difficult to reconstruct an experiment decades after the fact, we are fortunate that Lehman reported all of his data. A close inspection shows that the modulus and ultimate tensile strength were strongly correlated ( $p < 0.001$ ), with the higher values of elastic modulus associated with the specimens that had the highest tensile strength. Furthermore, 75% of the specimens failed in tension at or below 40 MPa, a low value suggesting that flaws introduced during specimen preparation may have affected the linear stress-strain behavior. When we restrict our focus to those specimens that failed above 40 MPa, we obtain a tensile modulus of 16.9 GPa with a coefficient of variation of 26%. This is more in line with the earlier work of Bowen and Rodriguez (1962).

Around the same time that the tensile measurements were being performed, other researchers were establishing the compressive properties of dentin. The earliest of these measurements was reported by Peyton *et al.* (1952). This study examined the compressive behavior of 1.8 mm in cross-section by 4.5-mm-long dentin specimens. Strain gauges were affixed to steel rods that were then used to apply load to the specimens. A Young's modulus of 11.6 GPa was reported.

Concerned that the low value of the Young's modulus obtained from their earlier study might have been caused by a combination of non-parallel alignment of the load platens (tow-in) and possible stress relaxation effects, the same group repeated their earlier study with greater attention to experi-

mental variables (Craig and Peyton, 1958). Placing the strain gauges directly on the specimen eliminated tow-in; stress relaxation effects were measured by careful cycling of the compressive load well below the proportional limit. These corrections raised the compressive Young's modulus to 18.5 GPa, in excellent agreement with the tensile measurements of the time.

Measurements of the modulus are sensitive to specimen preparation, experimental design, and stress relaxation; not accounting for these experimental variables leads to underestimation of the elastic constants. Therefore, the comments of Waters (1980) in his review article were surprising: "Craig and Peyton (1958) obtained values for the proportional limit and compressive strength in reasonable agreement with other workers, but their value of the modulus is, for some unaccountable reason, considerably higher." This comment reflects a bias toward favoring a low value for the Young's modulus of dentin—a bias perhaps enforced by the large number of low values reported in subsequent years (see Fig. 3).

Testing of dentin in compression and tension was performed only infrequently in the years since Craig and Peyton. Two of these studies are particularly noteworthy. In the work reported by Stanford *et al.* (1960), dentin specimens were tested in compression. Even with corrections for platen deformation, the compressive modulus was 13.8 GPa, significantly less than reported in the earlier studies. Though it could be argued that the data were not adjusted for the effects of non-parallel alignment (tow-in), it is unlikely that this could account for all of the discrepancy. Furthermore, in tensile testing performed by Sano *et al.* (1994), similarly low values of Young's modulus were reported (13-15 GPa).

Both of the above studies were performed with great attention to detail, so instrumentation artifacts or flaws in specimen preparation cannot readily explain the lower values of elastic modulus. However, one detail worth mentioning is that, in both studies, the specimens were stored for an undisclosed amount of time in water. In the work reported by Sano *et al.* (1994), the tensile specimens were stored in 0.9% NaCl water at 4°C for about 24 hrs prior to being tested (Pashley, 2001, personal communication). Earlier studies have showed that short-term storage in saline solution degrades bond strengths (Goodis *et al.*, 1993), and that storage in water can reduce bend strength in bone (Gustafson *et al.*, 1996). Given the small size of dentin specimens, it is possible that even short-term storage in water or saline might reduce the elastic modulus by dissolution of the mineral phase. The effects of water storage will be considered in greater detail later.

In more recent work, Palamara *et al.* (2000) recorded the response of a grid pattern coated on the surfaces of dentin specimens during compressive loading. The results are of particular interest because, while the Young's moduli measured in orientations both parallel and orthogonal to the tubule axes (the principal structural directions) were identical, the modulus at 45° off-axis to the tubules was determined to be lower. The observation that the off-axis modulus was smaller than that measured in either principal axis requires that the intertubular dentin matrix be anisotropic. Since this is a significant finding, we must consider its veracity in greater detail.

Our analysis begins by a consideration of the simplest deviation from isotropic symmetry, cubic, which requires three independent elastic constants. The reciprocal Young's modulus in a cubic system along the direction of the unit vector  $I_i$  can be expressed in terms of the compliance matrix  $S_{ij}$  (Nye, 1972):

$$S'_{11} = S_{11} - 2 \left( S_{11} - S_{12} - \frac{1}{2} S_{44} \right) (I_2^2 I_2^2 + I_2^2 I_3^2 + I_3^2 I_1^2) \quad (4)$$

The variation of the Young's modulus with orientation depends only on the terms in  $I_i$  and is zero for the principal orthogonal directions and a maximum of 1/3 in the <111> directions. For the Young's modulus to be less in the off-axis directions,  $(S_{11} - S_{12} - S_{44}/2)$  must be less than zero. This requires the shear modulus,  $G$ , to be less than would be expected in an isotropic system:

$$G < \frac{E}{2(1 + \nu)} \quad (5)$$

With the values provided by Palamara *et al.* (2000), [ $E_{11} = 10.4$  GPa and  $E(45^\circ) = 7.7$  GPa], we can calculate a rigorous upper bound for the shear modulus. For a cubic symmetry model,  $G < 2.9$  GPa. This is less than would be required from isotropic symmetry for  $\nu = 0.25$  (4.1 GPa).

One can argue that, from an analysis of the dentin microstructure, an orthotropic symmetry would be a more reasonable alternative to cubic. However, we find that the situation is only slightly altered from the analysis for cubic symmetry. For orthotropic symmetry, we begin with the general case of a lamina loaded in plane at an arbitrary angle  $q$  with respect to a principal axis,  $I_1$ , in this case parallel to the tubule axes. The Young's modulus as a function of  $q$  can be expressed as (Jones, 1975)

$$\frac{E_1}{E_q} = (1 + a - 4b)\cos^4(q) + (4b - 2a)\cos^2(q) + a \quad (6)$$

In Eq. 6,  $a$  and  $b$  are dimensionless variables given by

$$a = \frac{E_1}{E_2}$$

$$b = \frac{1}{4} \left( \frac{E_1}{G_{12}} - 2\nu_{12} \right) \quad (7)$$

Here,  $G_{12}$  is the shear modulus and  $\nu_{12}$  is Poisson's ratio. For the data presented in Palamara *et al.* (2000),  $a = 1$ . The observation that  $E_q$  was less than both  $E_1$  and  $E_2$  places a rigorous restriction on the value of the shear modulus:

$$G_{12} < \frac{E_1}{2(a + \nu_{12})} = \frac{E_1}{2(1 + \nu)} \quad (8)$$

The above restriction on the shear modulus is identical to the one derived for cubic symmetry. With the values reported in Palamara *et al.* (2000) for the off-axis Young's modulus, Eq. 6 requires that the magnitude of the shear modulus be less than 2.5 GPa, very similar to the result obtained with a cubic symmetry model. This is an extremely low value for the shear modulus, and is not in agreement with results reported in those studies where the shear modulus has been measured independently. Sound velocity measurements in bovine dentin, to be discussed in a later section, provided a shear modulus of 8.0 GPa (Gilmore *et al.*, 1969), and a torsion pendulum measurement led to a value

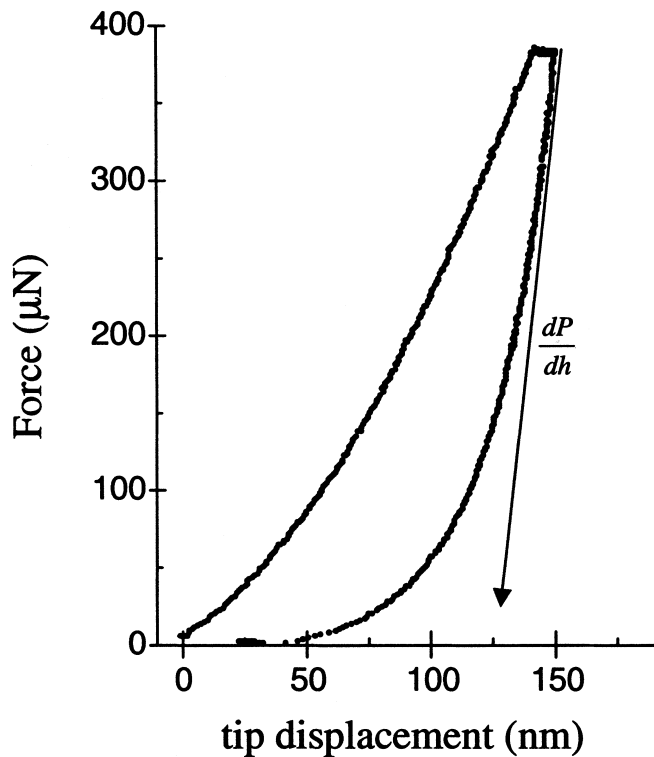


Figure 5. A typical load-displacement curve during AFM indentation of hydrated dentin. The slope of the initial unloading segment,  $dP/dh$ , is used to calculate the Young's modulus.

of 6.1 GPa (Renson and Braden, 1975). [NB: The value that we cite corrects the typographical error in the original paper by Renson and Braden (1975), where the decimal was placed in the wrong location.] These values were all significantly greater than what is required to explain the results of Palamara *et al.*

Though the largest source of error in measurements with grids lies in the accurate determination of displacement (strain), the absence of any independent measure of displacement (e.g., no strain gauges or cross-head displacements were reported) prevents us from assessing this as a possible source of error. However, the compression tests were conducted between 50 and 150 MPa, which is within the range of the proportional limit in compression (80-140 MPa) that has been established in earlier work (Craig and Peyton, 1958; Stanford *et al.*, 1960). It is therefore possible that Palamara *et al.* (2000) were operating beyond the yield stress when recording their grid displacements. This factor would explain the lower values of the Young's modulus, and could easily explain the off-axis anisotropy. Also, considerable relaxation (creep) could have occurred during the time intervals required to obtain the images of the grids. However, in the absence of additional data, the possibility that dentin is elastically anisotropic cannot be ignored. The question of elastic symmetry will be taken up again in a later section.

#### Indentation measurements of Young's modulus

Indentation, where a hardened stylus is brought into contact with a surface, has largely been used to measure hardness. The modern theory of indentation (Doerner and Nix, 1986; Oliver and Pharr, 1992), where force and stylus displacement are analyzed to measure Young's modulus, has been applied to mineralized tissues only in the last decade. The technique measures

the indenter load as a function of depth of penetration, from which the contact stiffness,  $S_c$  (not to be confused with the compliance matrix), is obtained from the derivative of the unloading curve evaluated at the peak force (Fig. 5). Care must be taken to remove any excess machine compliance,  $C_m$ , that is associated with the sample mounting (Kinney *et al.*, 1996):

$$S_c = \frac{1}{[(1/S) - C_m]} \quad (9)$$

The indentation modulus  $E^*$ , sometimes referred to as the reduced modulus, is determined from the corrected contact stiffness,  $S_c$  and the contact areas for each indentation,  $A$ , that are obtained from a tip shape calibration procedure (Doerner and Nix, 1986):

$$E^* = \frac{\sqrt{\pi}}{2\sqrt{A}} S_c \quad (10)$$

From Eqs. 9 and 10, it is possible to obtain the Young's modulus of the probed specimen,  $E_s$ :

$$\frac{1}{E^*} = \frac{(1 - \nu_s^2)}{E_s} + \frac{(1 - \nu_i^2)}{E_i} \quad (11)$$

$$E_s \cong E^* (1 - \nu_s^2)$$

In Eq. 11,  $\nu_s$  and  $\nu_i$  are the Poisson's ratios of the specimen and indenter stylus, and  $E_i$  is the Young's modulus of the indenter. The approximation in Eq. 11 is valid because the modulus of the indenter is considerably larger than the modulus of the dentin.

Among the first to apply nanoindentation to the study of dentin and dental materials was van Meerbeek *et al.* (1993), who measured a Young's modulus of dentin of 19.3 GPa. This was followed by Kinney *et al.* (1996), who used nanoindentation to measure the Young's modulus of intertubular (18-21 GPa) and peritubular (29.8 GPa). Since then, nanoindentation has become a common technique for the determination of local mechanical properties of structural features in biological hard tissues (Rho *et al.*, 1999).

A significant drawback to the widespread use of nanoindentation in mineralized tissues is the inability to indent in water. To overcome this drawback, Balooch *et al.* (1998) applied the atomic force microscope (AFM) with a specially designed attachment called the Triboscope to perform indentations on fully hydrated specimens. In addition to allowing indentations to be made in water, the device also functioned as an AFM, allowing for precise positioning of the indenter and subsequent imaging of the indentation with microscopic spatial resolution. With this technique, Kinney *et al.* (1999) measured a pronounced decline in  $E$  with submersion in water. These investigators attributed this decrease to a combination of softening of the collagen phase and partial surface demineralization. Without knowing the effects of surface demineralization, they assumed that a plasticizing of the collagen fibrils and other noncollagenous proteins in the tissue caused the majority of the decrease in modulus with time in water.

Although nanoindentation probes only a thin surface layer (< 1  $\mu\text{m}$ ), the mechanical properties obtained are assumed to be rep-

representative of the bulk material. Chemical changes in the surface layer of mineralized tissues resulting from storage solutions are, thus, important considerations for accurate determination of nanomechanical properties. This aspect of nanoindentation has been recently explored by Habelitz *et al.* (2002a), who studied changes in nanomechanical properties of dentin and enamel during storage in de-ionized water, calcium-chloride-buffered saline solution, and Hanks' Balanced Salt Solution (HBSS). The investigators were able to show that storing teeth in de-ionized water or CaCl<sub>2</sub> solution resulted in a large decrease in elastic modulus and hardness. After one day of storage, a decrease in the Young's modulus and hardness of up to 30% was observed. By one week of solution storage, mechanical properties dropped to below half of their initial values. In contrast, storing the specimens in HBSS did not significantly alter the mechanical properties for a time interval of two weeks. The behavior of the Young's modulus of specimens stored in water and HBSS is reproduced in Fig. 6.

The decrease in modulus and hardness of dentin when stored in de-ionized water or CaCl<sub>2</sub> solution was attributed to partial demineralization of the near-surface layer. Because de-ionized water lacks calcium and phosphate ions, the chemical potential for dissolution of the mineral phase of dentin and enamel is high, and was assumed to be the major reason for the demineralization and softening of the tissues. Addition of calcium chloride to a saline solution also did not prevent demineralization. Since the pH of the CaCl<sub>2</sub> solution was slightly acidic (pH = 5.9), it was more likely to dissolve the calcium phosphate minerals. HBSS, on the other hand, was slightly basic (pH = 8.0) and was unable to dissolve the mineral phases by acidic attack. It is highly concentrated in Ca<sup>2+</sup>, Mg<sup>2+</sup>, Na<sup>+</sup>, PO<sub>4</sub><sup>3-</sup>, and Cl<sup>-</sup> ions and has a composition comparable with that of the dental mineral phases. Therefore, the chemical potential of HBSS to dissolve the calcium phosphate phases in teeth is low, and surface demineralization was retarded.

By eliminating near-surface demineralization through proper specimen storage procedures, one can now obtain consistent values of the Young's modulus of hydrated peritubular and intertubular dentin. This is an important development, since it will allow for the study of the differences between wet and dry tissues, and provide elastic moduli more representative of *in vivo* conditions.

The nanoindentation method is limited in that it cannot be used to determine any of the other elastic constants, and it does not provide a direct measure of the continuum Young's modulus, since micromechanics arguments must be used to combine the separate measures of the inter- and peritubular dentin. Other techniques will now be described that have the potential to determine all of the second-order elastic constants of dentin completely.

### Sonic measurements of the elastic constants

Measurement of sound speed is among the most accurate ways of determining the elastic constants of a material. For an

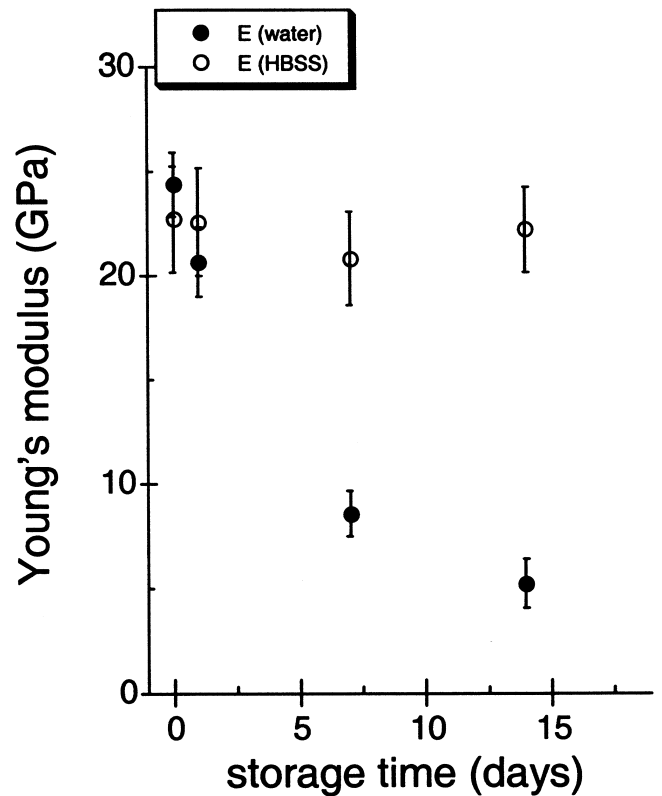


**Figure 6.** The Young's modulus of dentin as measured by AFM indentation. The solid circles represent repeated measurements obtained in water over the course of several days. The open circles show measurements obtained in Hanks' Balanced Salt Solution (HBSS). The water-stored specimens exhibited a rapid decline in modulus over 14 days. This decline was attributed to a loss of mineral from the near surface layer. The specimens stored in HBSS, in contrast, maintained relatively constant modulus values over the same time period. The error bars are the standard deviations of the means of several specimens. Data from Habelitz *et al.* (2002a).

isotropic material, the shear ( $G$ ), bulk ( $K$ ), and Young's ( $E$ ) moduli are related to the longitudinal ( $V_l$ ) and shear ( $V_s$ ) wave velocities and the specimen density,  $\rho$ , by (Love, 1960):

$$\begin{aligned}
 G &= \rho V_s^2 \\
 K &= \rho \left( V_l^2 - \frac{4}{3} V_s^2 \right) \\
 E &= \rho V_s^2 \left[ \frac{3V_l^2 - 4V_s^2}{V_l^2 - V_s^2} \right]
 \end{aligned}
 \tag{12}$$

**TABLE 1**

**The Elastic Moduli of Dentin as Determined by Measurement of Sound Speed (Gilmore *et al.*, 1969) and by Resonant Ultrasound Spectroscopy (RUS) (Kinney *et al.*, 2002)**

Method	$E_{11}$ (GPa)	$E_{33}$ (GPa)	$G_{23}$ (GPa)	$G_{12}$ (GPa)	$K$ (GPa)	$V_{21}$	$V_{31}$
Sound speed	19-29		7.2-10.8		18-29	0.32-0.34	
RUS (isotropic)	24.4		8.6		42.0	0.42	
RUS (hexagonal)	25.0	23.2	9.4	8.6		0.45	0.29

**TABLE 2**

**The Second-order Elastic Constants as Estimated from Critical Reflectance Ultrasound (Lees and Rollins, 1972) and by Resonant Ultrasound Spectroscopy (RUS) (Kinney *et al.*, 2002) for a Hexagonal Symmetry Model**

Method	$C_{11}$	$C_{12}$	$C_{13}$	$C_{33}$	$C_{44}$
Critical angle	37	16.6	8.7	39	5.7
RUS (hexagonal)	42.6	25.4	19.7	34.6	9.4

Using the technique of ultrasonic interferometry, Gilmore *et al.* (1969) established the sound speeds in bovine dentin. With these data, and assuming isotropic elasticity, the investigators used Eqs. 12 to derive the second-order elastic constants. To facilitate comparisons with other measurements, we have reproduced the entire range in values of the elastic moduli from this work (Table 1). The moduli, which are significantly higher than many more recent mechanical measurements, are in good agreement with nanoindentation (Habelitz *et al.*, 2002a).

The data from Gilmore *et al.* did not consider the possibility of anisotropy in the elastic constants. Lees and Rollins (1972) explored this possibility in a later study by measuring the longitudinal and shear wave velocities along orthogonal directions in the plane of the tubules. To facilitate these measurements, the investigators used the technique of critical angle reflection,

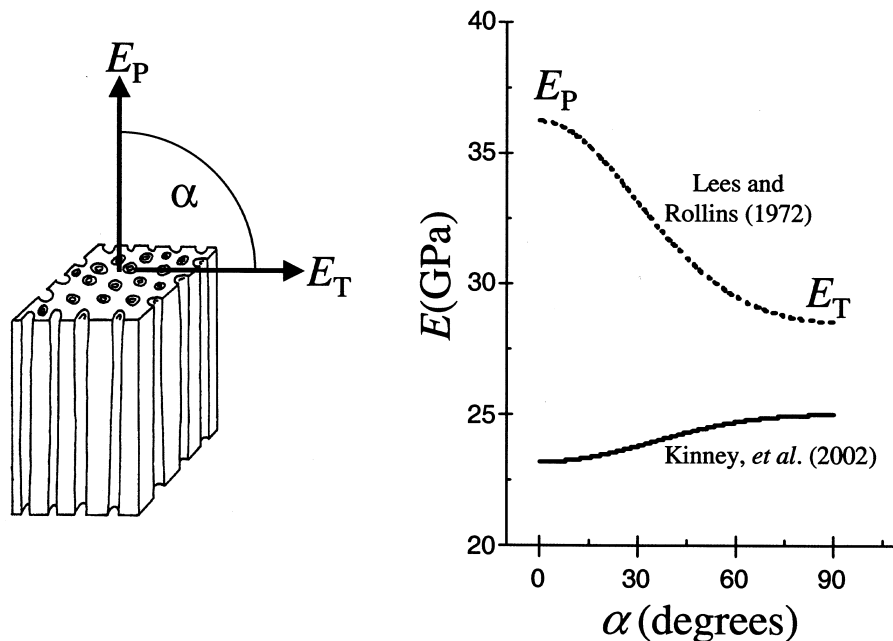


**Figure 7.** The Young's modulus of dentin as a function of orientation of the tubules as calculated from the elastic constants of Lees and Rollins (1972). There was a pronounced hexagonal (transverse isotropic) anisotropy in the Young's modulus, a result that was forced by a *priori* assumptions of the symmetry. The Young's modulus was greatest in the direction of the tubules (36 GPa) and much less in the orthogonal direction (29 GPa). The Young's modulus is compared with the values from the resonant ultrasound spectroscopy (RUS) measurements of Kinney *et al.* (2002). The RUS measurements, which were made without assumption as to material symmetry, also show hexagonal symmetry, but the stiffest orientation is now perpendicular to the axis of the tubules. This result is more consistent with what is known about the orientation of the collagen fibrils, which lie in a plane perpendicular to the tubule axis.

where the angle of incidence of the sonic wave is scanned while the intensity of the reflected wave is monitored simultaneously. At certain critical angles, determined by the shear and longitudinal sound speeds in the specimen, the refraction vanishes, and there is a local maximum in the reflected signal. With Snell's law, it is possible to calculate the longitudinal and shear wave speeds from the values of these critical angles.

The main difficulty with this method lies in determining the principal symmetry directions in the tooth from only two orientations. Lees and Rollins assumed hexagonal (transverse isotropic) symmetry based on the microstructure of dentin. However, since the elastic properties were measured in only a single plane, the solution to the stiffness tensor for hexagonal symmetry was underdetermined. Therefore, the investigators assumed that the lower-sound speed values reported earlier by Gilmore *et al.* were obtained from measurements  $45^\circ$  with respect to the tubule axes. With this assumption, the complete elastic stiffness matrix was estimated (Table 2).

Lees and Rollins (1972) reported only the magnitudes of the elements in their derived stiffness tensor ( $C_{ij}$ ). By matrix inversion, we can obtain the elements of the strain tensor, from which it is a simple task to calculate the Young's modulus. According to the hexagonal symmetry model and the stiffness tensor derived by Lees and Rollins, the Young's modulus in the tubule direction was 36 GPa, and 29 GPa in the perpendicular axis.

The Young's modulus, which can be derived from the stiffness matrix of Lees and Rollins (1972), is graphed in Fig. 7 as a function of tubule orientation. The transverse anisotropy in the critical reflectance data lies in contrast to what has been observed by either nano-indentation or compression testing along orthogonal axes. Also, the magnitude of the Young's modulus is significantly higher than that measured by Gilmore *et al.* Finally, the conclusion that the Young's modulus is higher in the direction of the tubules is at odds with both the micromechanics model, which dictates that the contribution to the elastic stiffness from the peritubular dentin should be negligible, and microstructural observations that the mineralized collagen fibrils lie perpendicular to the tubules.

In spite of the practicality of critical angle reflection methods, we must be skeptical of the conclusions. The chief criticism, one that was acknowledged by the investigators, was that the assumption that prior measurement made in different laboratories and using different methods corresponded to the local minimums in the hexagonal symmetry model. This assumption forces an anisotropy that may not be representative of the actual symmetry of the specimen. In fact, from our knowledge of bone, the modulus should be greatest in the direction of the collagen fibrils (Pidaparti *et al.*, 1996). In dentin, this would mean that the elastic modulus should be greatest in the direction perpendicular to the tubules, the complete opposite of the critical angle results. Therefore, we must consider the possibility that Lees and Rollins (1972)

made an incorrect assumption regarding the orientation of the specimens in the earlier work of Gilmore *et al.*

Clearly, what is needed is an ultrasonic method suited to small specimens, and which allows for the determination of all of the elastic constants from a single orientation of the specimen and without assumptions as to the symmetry. Indeed, these requirements are met by a technique known as resonant ultrasound spectroscopy.

Resonant ultrasound spectroscopy (RUS) is a method for measuring single-crystal elastic constants with great precision (Migliori *et al.*, 1993). RUS makes use of Hooke's law and Newton's second law to predict the resonant modes of vibration of a specimen of known shape (Migliori *et al.*, 1993; Maynard, 1996). The entire stiffness tensor,  $C_{ij}$ , can be determined by comparison of the frequency spectrum produced by the resulting eigenvalue problem with the measured resonant frequencies (vibrational eigenmodes) of the specimen. It is important to note a significant difference between RUS and other sonic methods. In RUS, sound speed is not measured. Rather, the resonant frequencies of mechanical vibration are determined. This means that the stiffness tensor can be determined for small specimens from one measurement at a single orientation.

Since the development of RUS, the applications of this technique have been extended to include geological structures and complex particulate and fiber-reinforced composites (Jung *et al.*, 1999). Recently, this technique has been applied to small specimens of human coronal dentin, with interesting results (Kinney *et al.*, 2002). Cubes of dentin, approximately 2 mm on an edge, were mounted on opposing corners between two transducers in the RUS system. The resonant frequencies between 0.5 and 1.4 MHz were measured. The values of the resonant frequencies were calculated from an initial approximation of the stiffness tensor. The experimental and predicted frequency distributions were then compared, and the residuals,  $F$ , were calculated. The elastic constants were adjusted from their initial values to minimize these residuals. Isotropic, cubic, and hexagonal material symmetry groups were modeled.

The elastic constants of hydrated and dry dentin, as measured by RUS, are listed in Table 1 for the isotropic, cubic, and hexagonal symmetry models. The best fit for the RUS data was with a hexagonal symmetry model, although deviations from isotropic symmetry were small. The angular deviation of the Young's modulus with respect to the axis of the dentinal tubules is graphed in Fig. 7. The Young's modulus was minimum in the direction of the tubules, and increased monotonically to maximum in the plane of the mineralized collagen fibrils. This should be compared with the critical angle results in the same Fig.

The measured anisotropy of the elastic constants of dentin can now be reconciled with its structural anisotropy. As in bone, the symmetry of the elastic constants is determined by the orientation of the collagen fibrils. However, the magnitude of the anisotropy (~10%) is not large. This may explain why previous studies have failed to detect anisotropic behavior in either the contact stiffness (Kinney *et al.*, 1999) or microhardness (Wang and Weiner, 1998a), since indentation techniques are known to be less sensitive to anisotropy (Vlassak and Nix, 1994). Furthermore, because the tubule orientation can vary widely across a specimen, a small anisotropy would most likely go undetected in a mechanical test of a larger specimen.

## Viscoelastic behavior of dentin

Thus far, we have assumed that dentin is perfectly elastic at small strains, and that the elastic constants do not depend on the strain rate. In other words, we have assumed that small deformations resulting from an imposed stress remain constant with time. In most biological tissues, this is not the case. At a constant stress, these materials continue to deform with time (creep). Therefore, if a constant strain is to be maintained, the applied stress must be continuously reduced (stress relaxation). Materials that exhibit a time-dependent response are called viscoelastic. If the time-dependence of the relaxation does not depend on the magnitude of the applied stress, the material exhibits linear viscoelasticity. On the other hand, if the time response changes with the applied stress, the material exhibits nonlinear viscoelasticity.

In a viscoelastic solid, the stress is out of phase with the strain. The amount of this phase shift is defined by a phase angle,  $\delta$ , between the applied stress and the resulting strain. A detailed analysis defines the loss tangent of the phase angle in terms of a storage modulus,  $E'$ , and a loss modulus,  $E''$ :

$$\tan(\delta) = \frac{E''}{E'} \quad (13)$$

In a perfectly elastic solid, there would be no energy lost to creep deformation ( $E'' = 0$ ), and the stress and strain would be in phase ( $\delta = 0$ ). With increasing viscoelastic behavior, the phase angle would increase due to an increase in  $E''$  and the corresponding decrease in  $E'$ . At extremely high strain rates (characteristic of ultrasound), or when stresses are too low to activate creep (typical of RUS), viscoelastic behavior should be less apparent. Therefore, the observation that the elastic constants determined by both RUS and sound velocity measurements are of similar magnitude, and that they are also higher than those determined by other methods, suggests that viscoelastic effects might contribute to the lower modulus values measured with mechanical testing. Indeed, Craig and Peyton (1958) measured a significant contribution from "stress-relaxation" during their compression loading studies, and nano-indentation measurements display continuous creep during the static load segment prior to unloading (*e.g.*, Kinney *et al.*, 1996; and also Fig. 5 in this review).

The classic analysis of viscoelasticity is based on the Maxwell element, a spring and dashpot arranged in series. The time-dependent relaxation modulus—for example,  $E(t)$ —can be written for a single element,  $i$ , as:

$$E(t) = E_i e^{-t/\tau_i} \quad (14)$$

where  $E_i$  represents the stiffness of the spring element  $i$ , and  $\tau_i$  is the relaxation time of the element. A parallel arrangement of a group of Maxwell elements can be treated as a simple sum:

$$E(t) = \sum_{i=1}^n E_i e^{-t/\tau_i} \quad (15)$$

For an infinite number of Maxwell elements, the relaxation modulus can be written as a function of the continuous relaxation spectrum,  $H(\tau)$ , and the reduced modulus at infinite relaxation time,  $E_0$  (Ferry, 1970):

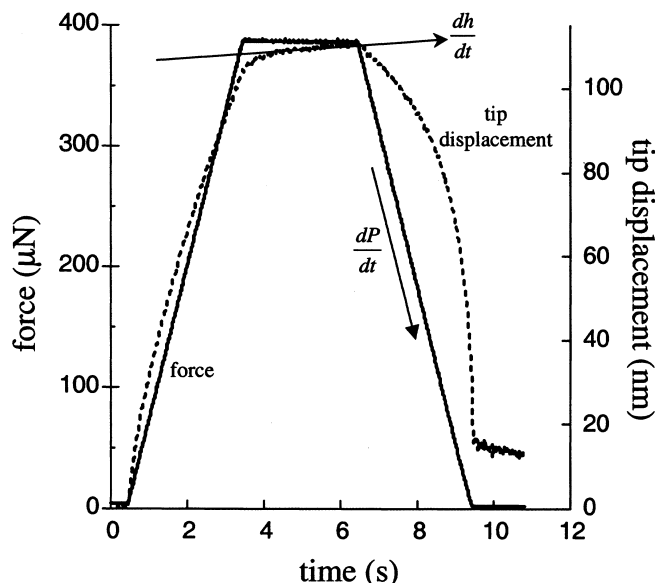


**Figure 8.** The applied force (solid line) and the tip displacement (dashed line) graphed as a function of time for a typical AFM indentation of hydrated intertubular dentin. In this example, the profile of the applied force was trapezoidal: a three-second loading phase, a three-second hold at maximum load, and a three-second unloading phase. At constant load, the indenter tip continues its inward displacement at a rate ( $dh/dt$ ) that is approximated by the slope of the dashed line at the midpoint of the hold phase. The unloading rate is given by  $dP/dt$ . These factors are used to correct the AFM data for creep relaxation. In this example, the correction to the contact stiffness raises the Young's modulus by about 20%.

$$E(t) = E_0 + \int_{-\infty}^{\infty} H(\tau) e^{-i/\tau} d \ln \tau \quad (16)$$

Similarly:

$$E'(\omega) = E_{\infty} + \int_{-\infty}^{\infty} \frac{H(\tau) \omega^2 \tau^2}{(1 + \omega^2 \tau^2)} d \ln \tau \quad (17)$$

$$E''(\omega) = \int_{-\infty}^{\infty} \frac{H(\tau) \omega \tau}{(1 + \omega^2 \tau^2)} d \ln \tau$$

A few studies have explored stress relaxation in dentin (Korostoff *et al.*, 1975; Tengrove *et al.*, 1995). Still, little is known about its time-dependent behavior. In what appears to have been the most detailed study of viscoelasticity in dentin, Korostoff *et al.* (1975) measured stress relaxation in specimens prepared from the roots of human incisors, cuspids, and premolars. The cylindrical specimens were machined to dimensions approximately 6.4 mm tall, and had a 3.8-mm outer and a 1.1-mm inner diameter. The specimens were loaded in compression at 37°C to a constant strain,  $\epsilon_c$ , of 0.6%. The relaxation modulus,  $E_r(t)$ , was determined from the experimentally observed drop in applied load,  $L(t)$ , and the change in specimen height,  $\Delta h_c$ :

$$E_r(t) = \frac{\sigma(t)}{\epsilon_c} = \frac{h_0 \sigma(t)}{\Delta h_c} = \frac{4h_0 L(t)}{\Delta h_c \pi (d_o^2 - d_i^2)} \quad (18)$$

In Eq. 18,  $h_0$  was the original specimen height, and  $d_o$  and  $d_i$  were the outer and inner specimen diameters, respectively.

Korostoff *et al.* (1975) observed an exponential decline in the relaxation modulus with time from the shortest time measured ( $t \sim 30$  sec) to a maximum relaxation time ( $t \sim 10^4$  sec). Beyond  $10^4$  sec, no further stress relaxation was detected. They established the fully reduced modulus,  $E_o$ , to be 12.0 GPa. The magnitude of the reduced modulus was as much as 40% lower than the instantaneous value at  $t = 0$ . This means that the Young's modulus measured by mechanical testing could range between 12 and 20 GPa, or greater, depending on the strain rate. Thus, it is probable that stress relaxation accounts for much of the discrepancy between mechanical testing and sonic measurements. This possibility can be explored more thoroughly by reconsideration of the AFM data.

It is well-known that the indenter stylus continues to displace inward during the constant load portion of an indentation measurement of dentin. This continued displacement is evidence that creep relaxation is occurring; the standard procedure for analyzing the indenter load/displacement data does not account for this relaxation. Recently, Feng and Ngan (2002) derived a correction formula for creep during indentation measurements. The correction is applied to the contact stiffness,  $S_m$ , measured at the beginning of unload:

$$\frac{1}{S_c} = \frac{1}{S_m} - \frac{\dot{h}_h}{|\dot{P}|} \quad (19)$$

In Eq. 19,  $S_c$  is the corrected contact stiffness to be used in Eq. 10, and the correction factor is the ratio of the time derivatives of the change in indenter displacement,  $h_h$ , during the constant hold cycle, and of the load,  $P$ , at the beginning of the unloading cycle.

This information has never been reported for indentation measurements on calcified tissues. However, approximate values for the correction factor can be obtained by estimation from the graphed representations of load and displacement with time. A graphed representation of both the stylus displacement and the load as a function of time is shown in Fig. 8. These data were obtained from a typical AFM indentation measurement on wet intertubular dentin (*e.g.*, Kinney *et al.*, 1999). We approximated the creep relaxation rate by taking the slope of the displacement vs. time at the midpoint of the unloading cycle (1.7 nm/sec in this example);  $dP/dt$  was approximated at a point midway between the maximum load and the minimum load during the unloading cycle (131  $\mu$ N/sec in this example). When the correction was applied to this specimen of wet dentin, the calculated Young's modulus increased from 20.6 GPa to 25.5 GPa, in excellent agreement with the RUS data (23.2-25.0 GPa; Table 1).

It now appears as if creep relaxation can explain the small differences between AFM indentation and RUS measurements of the modulus. However, the creep mechanisms, and their possible dependence on the magnitude of the applied stress, remain unknown. An important question, given the absence of a well-defined time-dependent equation of state, is, what values of the elastic constants should be used to describe elastic deformation that occurs under physiological loading conditions? For example, what magnitudes of the elastic constants should be used in the frequency range of physiological interest ( $\nu = 1 \text{ Hz} \sim 1/t$ )? This question can be answered only partially at this time.

A complete analysis of the time-dependent equation of state for dentin requires knowledge of the relaxation spectrum,

$H(\tau)$ , over all time scales. Then, the elastic constants can be formulated by expressions like Eq. 16. In principle,  $H(\tau)$  can be obtained by analysis of the stress relaxation data. Prior to availability of computers and digitally instrumented load frames, this procedure was complicated; approximations were used to derive  $H(\tau)$  from  $E(t)$ . For example, Korostoff *et al.* (1975) used an approximation method attributed to Alfrey and Doty (1945):

$$H(\tau) \cong \left[ \frac{-dE(t)}{d \ln(t)} \right]_{t=\tau} \quad (20)$$

With this approximation, Korostoff *et al.* (1975) evaluated the relaxation spectrum for root dentin for relaxation times from 30 sec to  $\sim 10^4$  sec. The important result was the finding that the relaxation spectrum was constant over the three decades examined. Though the magnitude of  $H$  varied among specimens ( $H = 0.38$  MPa;  $SD = 0.14$ ), it was in all cases independent of the relaxation time. This was an important result; a constant value of  $H$  greatly simplifies the evaluation of the integral relationships in Eqs. 16 and 17.

There were admitted shortcomings with the study. Most critical, no information was provided about stress relaxation at time scales shorter than 30 sec. Physiological time scales of greatest relevance lie in the range of 0.1 to 10 sec. There is a serious concern with extrapolating the above results to shorter time scales. In bone, deviation from simple exponential relaxation has been observed; stress relaxation at short time scales has followed a Kohlrausch-Williams-Watts (KWW) functional form (Sasaki *et al.*, 1993). Much more research, particularly at short time scales, is warranted.

No one has measured the frequency dependence of the loss tangent (Eq. 13) for dentin. In the absence of this information, it is instructive to consider bone, which is compositionally similar to dentin. In a series of classic articles, Lakes and Katz (1979) provided the loss tangent in wet cortical bone over eight decades in relaxation time. Of interest was the observation that the loss tangent was a minimum, and also relatively constant, at physiologically relevant frequencies. If similar behavior can be inferred for dentin, then it would be reasonable to treat the dental hard tissues as perfectly elastic in physical models of mechanical deformation at physiologic strain rates, using, of course, the reduced values of the storage and loss moduli. More study is needed.

## SUMMARY OF ELASTIC PROPERTIES

The good agreement between indentation and sonic measurements of the Young's modulus of hydrated dentin allows us to assign its magnitude between 18 and 25 GPa. The bottom of this range (18-20 GPa) is probably more appropriate for strain rates encountered with physiologic loading. This is significantly greater than the previously accepted range (13-16 GPa). However, the larger Young's modulus is now more consistent with what has been observed in bone, a mineralized tissue of similar composition. Smaller values of the Young's modulus that are frequently reported can most likely be attributed to a strain-rate-dependent viscoelastic response, non-uniform stress states in small specimens, improper storage conditions, or flaws introduced during specimen preparation.

Sonic methods provide the most direct and precise determination of the elastic constants. They are least affected by stress relaxation. Because of this, we propose that the data

from the RUS (Kinney *et al.*, 2002) and sound speed measurements (Gilmore *et al.*, 1969) be used to define the most probable range for all of the elastic constants of dentin in the absence of viscoelastic effects (Table 1). Because RUS is more likely to probe perfectly elastic behavior (the maximum strain in the specimen was  $6 \times 10^{-6}$ , and the Mach number was approximately  $1.4 \times 10^{-5}$ ), and because RUS does not require assumptions as to the material's symmetry, we believe them to be the most accurate values of the elastic constants yet measured. However, because RUS has been applied only to coronal dentin from a single site, one should refrain from generalizing these results. It is probable that the elastic properties are site-dependent. Much more work remains to be done.

The intrinsic elastic constants provide only part of the story. The viscoelastic behavior of dentin must be explored in greater detail if a constitutive equation of state is to be developed for dentin. In the frequency range of physiological interest (0.1-10 Hz), the phase angle between stress and strain is most likely small, so that dentin can be modeled as a perfectly elastic solid. However, it is likely that the effective elastic moduli are reduced by about 10-20% from the values obtained with sonic measurements. This is consistent with the differences between the RUS measurements and those obtained by indentation and uni-axial testing. However, this observation is still speculative: The mechanisms controlling viscoelastic behavior, and their possible dependence on the stress amplitude, remain unknown in dentin.

As our knowledge of the elastic properties of normal dentin improves, other questions are raised that have significant implications for dentin pathologies. Is there a functional relationship between the mineral density and the elastic moduli? Does age-related transparency alter the elastic properties of root dentin? Does reparative dentin that forms at the dentin/pulp interface have the same elastic properties as the secondary dentin it adjoins? Answers to these questions will be important in the continued development of minimally invasive approaches in restorative dentistry.

## Hardness of Dentin

Hardness tests measure the resistance of the dentin to deformation caused by penetration of an indenting stylus. Since its introduction, the Knoop (Knoop *et al.*, 1939) indenter has proved to be the workhorse in studies of dentin. The long aspect ratio (7.11 times longer in one dimension) allows for accurate measurements of area, even with shallow indentations. Knoop, therefore, is extremely useful for the small, thin specimens typical of studies of mineralized tissues.

Hardness is defined in units of pressure, or force *per* unit area of indentation. Unlike Vickers or Brinell methods, which use the contact area of the indenter stylus, the Knoop method uses the projected area,  $A_p$ , in the calculation of hardness (KNH):

$$KNH = \frac{P}{A_p} = 14.22 \frac{P}{l^2} \quad (21)$$

where  $P$  is the applied load (in kg) and  $l$  is the length (in mm) across the long axis of the remnant impression. In SI units,  $1 \text{ kg/mm}^2 \sim 9.8 \text{ MPa}$ .

Many investigators have determined that dentin hardness depends on mineral concentration. Featherstone *et al.* (1983) developed an analytic expression relating Knoop hardness to

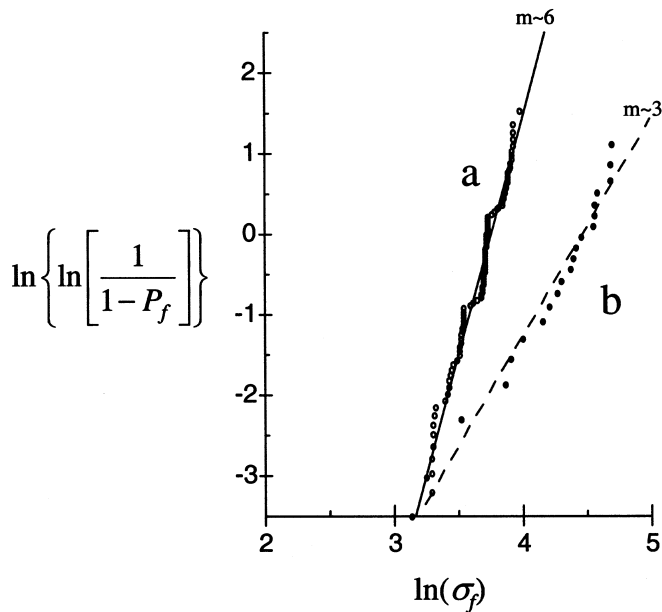


**Figure 9.** Ultimate tensile strength data from Lehman (1967) (open circles) and Staninec *et al.* (2002) (solid circles). The data have been graphed in the form of a Weibull probability distribution function, with the abscissa given by the natural log of the failure stress, and the failure probability,  $P_f$ , given by Eq. 23. Both sets of data fit the Weibull distribution function ( $R^2 = 0.97$ ), although the slopes,  $m$ , are different. The slope of the curve determines the sensitivity of the tensile strength to specimen size. Weibull behavior is an indication that a distribution of flaws determines the magnitude of the tensile strength of dentin.

the volume percent of mineral ( $V_m$ ):

$$\sqrt{KNH} = 0.197V_m - 0.24 \quad (22)$$

Though the validity of Eq. 22 obviously breaks down for low concentrations of mineral, the expression appears to fit the experimental data over a range of mineral concentrations associated with normal and carious dentin.

In addition to its association with the mineral concentration, hardness has been correlated with location in the tooth. The works of Ogawa (1983) and Wang and Weiner (1998b) show that the mantle dentin immediately subjacent to the enamel ( $KNH \sim 60 \text{ kg/mm}^2$ ) is softer than the underlying primary dentin ( $KNH \sim 70 \text{ kg/mm}^2$ ). Also, hardness gradually decreases with proximity to the pulp, falling precipitously in an inner layer of dentin of about 0.5 mm thickness that surrounds the pulp ( $KNH \sim 30 \text{ kg/mm}^2$ ).

Clearly, Eq. 22 mandates that  $V_m$  must be lower near the pulp than in the primary dentin. However, whether this is a result of increased porosity, or whether the intertubular dentin matrix is less mineralized, is an important question. In a careful and methodical study, Pashley and Parham (1985) determined that there was a significant correlation between decreased hardness and increased density of tubule lumens. The authors concluded that the reduced hardness was an end result of the lower mineral concentration brought about by the increased tubule porosity. This conclusion, however, was seriously challenged in a later study by Kinney *et al.* (1996), who showed that most, if not all, of the decreased hardness near the pulp could be explained by a decrease in the hardness of the

intertubular dentin matrix. Thus, it is likely that the intertubular dentin matrix near the pulp is less mineralized.

It is tempting to try to relate dentin hardness to other physical properties like yield stress, tensile strength, or Young's modulus. In ductile metals, for example, the yield stress and tensile strengths are often observed to scale with hardness. However enticing these scalings, we must remember that they were derived from plasticity theory for materials that display significant yielding. In contrast, mineralized tissues are more brittle, showing little if any yielding prior to failure.

Though we should not anticipate similar relationships with dentin hardness, there is a possibility that its hardness might scale with the Young's modulus. Eq. 22 describes a relationship between hardness and mineral concentration, and there is strong evidence that the Young's modulus is also dependent on the amount of mineral. However, because hardness also depends on yielding, microstructural features in the dentin that do not influence the elastic properties might mask any such correlation. In many materials, for example, the grain size controls yield strength by the Hall-Petch relationship. Therefore, the ratio of hardness to modulus need not be constant. Nevertheless, a relationship between hardness and modulus in dentin is worth seeking. Although several papers have reported hardness and modulus values for enamel and dentin, a systematic analysis of their relationship has not been undertaken.

### Ultimate Strength of Dentin

Failure data have largely been limited to measurements of shear strength or ultimate compressive or tensile strength. For dentin specimens failed in tension, reported magnitudes of the ultimate strength range from 52 MPa (Bowen and Rodriguez, 1962) to 105 MPa (Sano *et al.*, 1994). It is likely that the two-fold differences in the tensile strength were related to flaws in the specimens, since both a size effect and an improvement in strength with surface sanding of the specimens have been noted (Sano *et al.*, 1994). Moreover, measurements of compressive strength, which are less likely to be affected by flaws, were more consistent. Values of compressive strength range from 275 to 300 MPa (Craig and Peyton, 1958).

Shear strength, measured either by punching or lap-shear, also has been highly variable. Using a shear punch apparatus, Cooper and Smith (1968) obtained values for shear strength that ranged from 64 to 132 MPa, not too dissimilar from later measurements by Roydhouse (1970) (69-147 MPa). More recent measurements by single-plane lap shear produced shear strengths of 36 MPa; this low value may have been due to the specimens having been from dentin closer to the pulp, or to problems with the experimental design, or with bending of the specimen (Gwinnett, 1994).

Our group (Watanabe *et al.*, 1996) demonstrated that some of the disparity in reported values of the shear strength could be attributed to tubule orientation and location within the tooth. The lowest values of lap shear strength were obtained in less mature dentin nearer the pulp, with the tubules oriented parallel to the shear plane (54 MPa). The highest values were obtained in mature cuspal dentin with the shear plane perpendicular to the tubules (92 MPa). Others also have observed a similar orientation dependence with the tensile strength (Lertchirakarn *et al.*, 2001).

The large standard deviations common to all measurements of dentin strength suggest that strength is controlled by the flaw distribution in a specimen. A flaw is similar to the

weakest link in a chain: Variations in the flaw size lead to variations in the failure strength. Specimens with large flaws will fail at lower stresses than will specimens containing smaller flaws. For a random distribution of flaws, the tensile strength should obey a Weibull probability distribution function (pdf), where the probability,  $P_f$ , that a specimen fails at a stress level  $\sigma$  is given by the expression:

$$P_f = 1 - \exp\left(-V\left(\frac{\sigma}{\sigma_0}\right)^m\right) \quad (23)$$

In Eq. 23,  $V$  is the volume of the gauge region of the specimen,  $\sigma_0$  is the shape factor, and  $m$  is the dimensionless Weibull modulus. A specimen size effect follows naturally from the Weibull pdf. For two specimens with identical flaw distributions, the failure strengths will scale with the respective volumes ( $V_1$  and  $V_2$ ) of the gauge region as:

$$\frac{\sigma_1}{\sigma_2} = \left(\frac{V_2}{V_1}\right)^{1/m} \quad (24)$$

The Weibull modulus,  $m$ , determines the size-sensitivity of the failure strength; smaller values of  $m$  lead to greater sensitivity to specimen size.

Most studies of tensile strength have recorded only the means and standard deviations of the experimental measurements. An exception was the early work of Lehman (1967), who tabulated the test results of all 100 of his tensile strength measurements of root dentin. These results are recast in a Weibull distribution in Fig. 9. Included for comparison are the tensile strength results from mid-coronal dentin reported by Staninec *et al.* (2002). Both data sets are well-described by the Weibull distribution function ( $R^2 = 0.97$ ). However, the Weibull moduli are different for the two examples shown ( $m \sim 6$  for Lehman's data;  $m \sim 3$  for the displayed example from Staninec *et al.* [2002]). Staninec *et al.* observed that the Weibull modulus did not vary statistically with depth or location in the tooth; the average Weibull modulus was 4.5, with a range between 3 and 6. The large variations in the Weibull modulus may reflect differences in the flaw population between teeth, or may simply be the result of random defects introduced during specimen preparation. It has also been suggested that the Weibull modulus might decrease with age, reflecting an age-related change in either the distribution of flaws or their stress-sensitivity (Tonami and Takahashi, 1997). The flaws are cryptogenic; the precise nature of these flaws, whether they are intrinsic to dentin or created in specimen preparation, needs to be determined.

### Fracture Properties of Dentin

The previous discussion of dentin strength suggests that a fracture mechanics approach would be more appropriate than a strength-of-materials approach for the study of tooth failure. Yet, surprisingly few studies have taken this approach. Important exceptions to an otherwise-absence of quantitative fracture data are the works by Rasmussen *et al.* (Rasmussen *et al.*, 1976; Rasmussen, 1984; Rasmussen and Patchin, 1984), El Mowafy and Watts (1986), and Imbeni *et al.* (2002). Rasmussen *et al.* determined the work-of-fracture of normal dentin in directions parallel and perpendicular to the tubule axis. This work was important in that it detected a small directional dependence in the work-of-fracture; it was energetically more favorable to

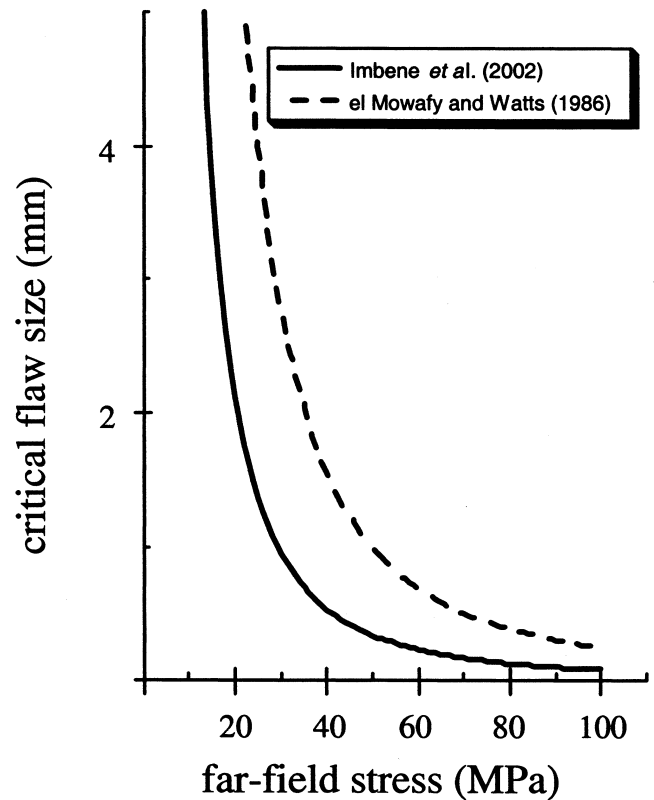


Figure 10. The critical flaw size in dentin as a function of far-field applied stress (MPa). The critical flaw size is calculated for an elliptical flaw according to Eq. 25. The dashed line corresponds to the fracture toughness established by El Mowafy and Watts (1986):  $K_{Ic} = 3.08 \text{ MPa} \sqrt{m}$ . The solid line corresponds to the more conservative estimate of the fracture toughness determined by Imbeni *et al.* (2002):  $K_{Ic} = 1.8 \text{ MPa} \sqrt{m}$ . Knowledge of the critical flaw size is of great importance in lifetime modeling.

fracture dentin perpendicular to the axis of the tubules than parallel to them. However, the relatively large works-of-fracture implied a toughening mechanism and the possibility of significant yielding ahead of the crack. Perhaps because of this, the authors stopped short of equating the work-of-fracture with any intrinsic material property such as fracture toughness.

The work by El Mowafy and Watts (1986) was of considerable importance. It was the first attempt to measure the intrinsic fracture toughness,  $K_{Ic}$ , of dentin with an ASTM standard specimen geometry: the compact tension specimen. For normal coronal dentin, these investigators reported a value of  $3.08 \text{ MPa} \sqrt{m}$  with a 10% standard deviation. Based upon an unpublished value of the yield stress, the authors assumed that the test resulted in a valid measure of  $K_{Ic}$ . They could therefore equate their fracture toughness measures with the energy release rate,  $G$ , and obtained good agreement with the earlier data of Rasmussen (Rasmussen *et al.*, 1976; Rasmussen, 1984; Rasmussen and Patchin, 1984).

Three valuable findings came from the work of El Mowafy and Watts (1986): (1) Compact tension specimens could be fabricated from coronal dentin; (2) fracture toughness was high for a brittle material, indicating that either the collagen fibrils or the tubule lumens provide a toughening mechanism; and (3) fracture toughness was independent of temperature through a range

from 0 to 60°C. However, since the fracture plane was parallel to the tubules (*i.e.*, in the orientation associated with the highest work of fracture), it is possible that the fracture toughness could be considerably lower in the orthogonal plane. Furthermore, El Mowafy and Watts (1986) used a blunt notch instead of a fatigue precrack, so that notch toughening might have elevated their results. To explore these possibilities further, Imbeni *et al.* (2002) considered the effects of notch root radius on the measurement of fracture toughness in a direction perpendicular to the tubules.

Imbeni *et al.* (200) prepared 10-mm-long beam-shaped specimens from human molars. Tests were conducted in three-point bend, with a span between the loading points of approximately 5 mm. Two protocols were followed. For the first protocol, sharp notches were prepared in the specimens with the root radius ranging from 30 to 50  $\mu\text{m}$ . For the second protocol, a fatigue precrack was grown out of the notch by fatigue cycling at 2 Hz with a maximum stress intensity of about 1 MPa  $\sqrt{m}$ . The fracture toughness in the fatigue-precracked specimens was 1.8 MPa  $\sqrt{m}$  (SD = 0.1), whereas, in the notched specimens, the fracture toughness was significantly higher (2.7 MPa  $\sqrt{m}$ ; SD = 0.1). Upon further analysis, these authors found evidence of an apparent relationship between the fracture toughness and the square root of the notch radius.

Was the lower value of the fracture toughness measured in Imbeni's work entirely the consequence of their having used a fatigue precrack, or was it also affected by the orientation of the fracture plane? This is important, since the critical flaw size,  $a_c$ , is a strong function of the fracture toughness  $K_c$ :

$$a_c \propto \frac{K_c^2}{\pi \sigma_{app}^2} \quad (25)$$

If the difference in fracture toughness was an artifact of the notch radius, then for the same far-field applied stress,  $\sigma_{app}$ , the critical flaw size would be roughly three times smaller than that predicted from the earlier values of El Mowafy and Watts (1986). The critical size of an elliptical flaw is graphed as a function of the far-field stress in Fig. 10. Since the critical flaw size has a profound importance on lifetime modeling (see following section), answers to these questions are needed.

### Fatigue Properties of Dentin

Teeth are subject to cyclic loads during mastication. The frequency of the loading is nominally 1 Hz, and stress amplitudes of 20 MPa can be estimated at the cervical margins (Anderson, 1956). Therefore, it is important to know the response of the tooth to cyclic loading: its fatigue behavior. Characterizing fatigue behavior involves determining the total life to failure in terms of a cyclic stress range. This method is often referred to as the "S/N" (stress/life) approach, and requires the measurement of the number of cycles required to induce failure in a flaw-free material at a given alternating stress. Some materials exhibit a fatigue limit: a stress below which failure does not occur. Many materials, however, do not have a fatigue limit. For those cases, it is convenient to define a material lifetime in terms of the endurance strength, which is the alternating stress below which the material will not fail before a predefined number of cycles.

Does dentin exhibit classic S/N behavior, and, if so, are the cyclic stresses of mastication below its endurance strength? A partial answer to this question was provided in a study of ten-

sile fatigue behavior in bovine dentin (Tonami and Takahashi, 1997). In that study, tensile specimens with 1.5 x 1 x 1-mm-gauge sections were subjected to a sinusoidal cyclic unipolar load at 5 Hz. The load ratio, R, which is defined as the minimum load divided by the maximum load, was allowed to vary between 0.15 and 0.25. A staircase method was used to determine the stress at which the specimen failed at  $10^5$  cycles. For example, if a specimen did not fail at  $10^5$  cycles at a stress of 45 MPa, another specimen was tested at a stress level 5 MPa higher. With this procedure, Tonami and Takahashi (1997) established the endurance strength, for failure at  $10^5$  cycles, to lie between 45 and 50 MPa. This would suggest that fatigue is not a factor in tooth failure under conditions of normal masticatory loading.

The work of Tonami and Takahashi was important in establishing the existence of fatigue failure in dentin. However, there were several shortcomings that limit its usefulness. First, the endurance strength was established for failure at  $10^5$  cycles. This was short, especially considering that  $10^6$  cycles are expected in a year from mastication. Second, the load frequency used in the study (5 Hz) was five times greater than that observed in physiological loading (1 Hz); the investigators assumed that there would be no frequency dependence on the fatigue life. This was a questionable assumption, however, especially considering the pronounced frequency dependence of fatigue in bone (Ziopoulos *et al.* 2001). Finally, the work was performed on bovine dentin.

The recent work of Nalla *et al.* (2002) was designed to address many of these issues. In this study, specimens of human dentin were subjected to fatigue loading at a constant load ratio, R = 0.10, and at two different cyclic frequencies: 2 and 20 Hz. The authors observed the existence of a classic S/N fatigue response to repetitive loading, and identified an apparent fatigue limit at  $10^6$ - $10^7$  cycles, which was estimated to lie between 25 and 45 MPa at frequencies of 2 and 20 Hz, respectively. Failure appeared to be caused by the initiation and growth of a single, dominant crack.

In the absence of intrinsic flaws, it appears that fatigue failure will not occur in human teeth. However, the Weibull nature of tensile failure indicates that there is an inherent population of pre-existing flaws in normal dentin. Thus, the existence of a fatigue limit in a nominally flaw-free specimen of dentin cannot be generalized to the whole tooth. The classic S/N approach is not conservative enough; it does not address the question of whether a pre-existing flaw can grow to a critical size during normal loading conditions. This requires the measurement of fatigue growth crack rates,  $da/dN$ , for a fracture-mechanics-based approach to failure of human dentin.

Nalla *et al.* (2002) determined the fatigue crack growth rate by measuring stiffness loss in the specimen during cyclic loading. They observed a Paris power law relationship of the crack growth rate with the stress intensity,  $\Delta K$ . The experimentally derived crack growth rate for human dentin was determined to be:

$$\frac{da}{dN} = C(\Delta K)^m = 6.24 \times 10^{-11} (\Delta K)^{8.76} \quad (26)$$

The Paris law exponent,  $m = 8.76$ , was smaller than that of carbonated apatite bone substitute ( $m = 17$ ; Morgan *et al.* 1997), but larger than that frequently observed in ductile metals ( $m \sim 2$ -4; Ritchie, 1999). The Paris power law relationship provides a

method for estimating a threshold stress intensity,  $\Delta K_{TH}$ , below which crack growth cannot occur. Extrapolation of Eq. 26 yielded a threshold stress intensity of  $1.1 \text{ MPa } \sqrt{m}$ . For stress intensities greater than  $\Delta K_{TH}$ , subcritical crack growth will occur.

When a crack reaches a critical size,  $a_c$ , determined by equating the fracture toughness,  $K_c$ , with the stress intensity at the crack tip, the structure will fail. Nalla *et al.* (2002) used lifetime modeling to estimate the number of cycles,  $N_f$ , required for an incipient crack of length  $a_o$  to grow to the critical size under a far-field applied stress  $\Delta\sigma_{app}$ :

$$N_f \approx \frac{2(f(a/b)\Delta\sigma_{app})^{-m} \pi^{-m/2} [a_o^{1-m/2} - a_c^{1-m/2}]}{(m-2)C} \quad (27)$$

In Eq. 27,  $m$  and  $C$  were determined from the experimental data (Eq. 26); the dimensionless function  $f(a/b)$  was determined for a small, elliptical surface flaw; for this configuration,  $f(a/b)$  was equal to 1.12.

Eq. 27 was an important result. Now it was possible to estimate the number of cycles (time) required for an incipient crack to reach catastrophic proportions. It also placed a limit on the necessary spatial resolution of a clinical imaging system to detect the smallest flaw size that could eventually grow large enough to cause failure. In a hypothetical example, consider the smallest crack that could grow to critical size in a year's time as a result of mastication forces of 20 MPa ( $\sim 10^6$  cycles). With a conservative estimate of  $K_c$  of  $1.8 \text{ MPa } \sqrt{m}$ , the critical flaw size is about 2 mm. Eq. 27 predicts that a 0.9-mm crack would grow to critical size in  $10^6$  cycles. If the mastication forces were even higher, say 30 MPa, a pre-existing crack of 0.3 mm would grow to critical size in the same number of cycles (see Fig. 11). Whereas the classic S/N approach predicts that fatigue failure cannot occur at stresses below 30 MPa, this more conservative damage-tolerant approach suggests that failure will occur at these stresses if there were a pre-existing flaw of sufficient size. The source of these flaws remains unknown; their existence can be inferred from the statistical nature of tensile failure.

Two major assumptions have gone into the development of Eq. 27. First, the crack growth rate was inferred from stiffness loss in the specimens during cyclic loading. If there were a sizeable yield, or damage, zone ahead of the crack tip, its contribution to the stiffness loss would affect the estimate of the crack length. Second, and perhaps more serious, is the fact that the crack growth rate measurements were performed in a controlled environment of Hanks' balanced salt solution. It is quite possible that the fluctuations of pH and mineral concentration in the mouth might have a pronounced effect on crack growth rate. Further study of environmental effects on fatigue crack growth is warranted.

### Conclusions

Many of our conceptions of basic biomechanical properties of dentin have changed since the last comprehensive review (Waters, 1980). The magnitudes of the elastic constants must be revised upward, and viscoelastic effects must be taken into account. Also, the concept of strength as an important engineering quantity must be replaced by a fracture mechanics approach to dentin failure, since pre-existing flaws can cause teeth to fail at stresses far less than their theoretical strength. In particular, a lifetime modeling, or damage-tolerant, approach

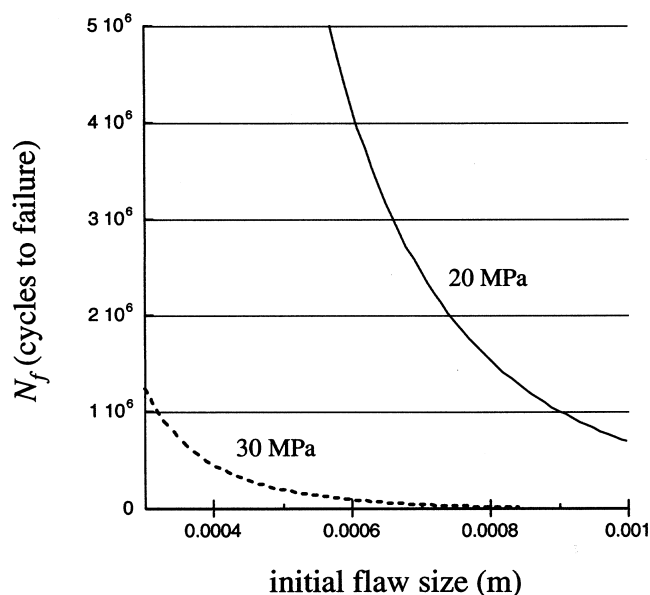


**Figure 11.** The number of required cycles for growing a flaw from an initial to critical size for two different far-field stresses (Eq. 27). The solid line is for a far-field stress of 20 MPa; it corresponds to the stresses of mastication. The dashed line corresponds to a slightly elevated stress level (30 MPa). An initial flaw 0.3 mm long will grow to catastrophic size in roughly  $10^6$  cycles at 30 MPa (approximately one year); at 20 MPa, a pre-existing flaw would have to be 0.9 mm long to grow to catastrophic size in the same number of cycles. Lifetime models such as Eq. 27 depend critically on the Paris law exponent,  $m$  (Eq. 26), the critical flaw size (Eq. 25), and the stress intensities at the head of the crack tip.

appears promising for the development of a clinical predictor of tooth failure. These paradigm shifts have been facilitated by advances in measurement science combined with a better understanding of dentin microstructure.

It now appears that the elastic constants of dentin have hexagonal symmetry, with the stiffest direction oriented in the plane perpendicular to the tubules. This finding is consistent with a micromechanics model that suggests that the peritubular dentin has negligible influence on material symmetry. Furthermore, it is also consistent with the observations in other tissues that the stiffest orientation is in the direction of the mineralized collagen fibrils. We can conclude, then, that the elastic properties of dentin are explainable in terms of the microstructure of the intertubular dentin matrix, and that any correlation of the elastic properties with the tubule direction is a necessary consequence of the orthogonal relationship between the tubules and collagen fibrils. Therefore, research must focus on the mineralized collagen scaffold, and explore the coupling between the mineral and collagen phases and its effects on biomechanical properties.

The Weibull behavior of tensile strength data suggests that failure initiates at flaws. These flaws may be intrinsic, perhaps regions of altered mineralization, or extrinsic, caused by cavity preparation, wear, or damage. Clearly, identifying the flaws responsible for failure is important, as is the understanding of how sub-critical flaws can grow and coalesce with cyclic loading. Though the cyclic forces of mastication are insufficient to cause failure in perfect dentin, it now appears that pre-existing

flaws in normal dentin can grow to catastrophic size with application of small cyclic loads. Furthermore, understanding how shifts in the chemical environment affect the crack growth rate will be essential for developing lifetime models. At present, many of these data are lacking.

Finally, little is known about the biomechanical properties of altered forms of dentin. Studies seem to suggest that there are at least two forms of transparent dentin, a form associated with caries and a form associated with age-related changes in the root. Each type of transparency may exhibit unique biomechanical signatures. In addition, there are caries lesions and genetic disorders, such as dentinogenesis imperfecta, which appears to lack the phosphoproteins that promote binding between the mineral and the collagen. It is absolutely essential that the properties of these altered forms of dentin be obtained before an understanding of how dentin pathologies affect tooth strength can be developed.

Current conservative dental practice is increasingly oriented toward efforts to arrest and remineralize caries lesions with either solution chemistry or more fundamental tissue engineering approaches. An accurate understanding of the properties of the dental hard tissues is a requirement for assessment of the effectiveness of these approaches. Without knowledge of mineral-collagen coupling and its biomechanical consequences, we may not truly be restoring the affected tissues. This shift in emphasis from traditional filling procedures to tissue restoration requires a firm understanding of the structure/properties relationships in dentin at many length scales. It is hoped that this review has clarified what is known, and has raised awareness of what remains to be learned about the mechanical properties of dentin.

### Acknowledgments

This work was supported in part by the National Institutes of Health, National Institute of Dental and Craniofacial Research (grants PO1 DE09859, DE 11526, and DE13029). The authors thank many investigators for sharing their time, comments, and data prior to publication. In particular, we thank Prof. David Pashley, Prof. Lawrence Katz, Prof. Robert O. Ritchie, Dr. James S. Stolken, Dr. Stefan Habelitz, and R.K. Nalla for valuable discussions.

### REFERENCES

- Alfrey T, Doty P (1945). The methods of specifying the properties of viscoelastic materials. *J Appl Physics* 16:700-713.
- Anderson DJ (1956). Measurement of stress in mastication. *J Dent Res* 35:664-670.
- Balooch M, Wu-Magidi IC, Balazs A, Lundkvist AS, Marshall SJ, Marshall GW, et al. (1998). Viscoelastic properties of demineralized human dentin measured in water with atomic force microscope (AFM)-based indentation. *J Biomed Mater Res* 40:539-544.
- Bonar LC, Lees S, Mook HA (1985). Neutron diffraction studies of collagen in fully mineralized bone. *J Molec Biol* 181:265-270.
- Bowen RL, Rodriguez MM (1962). Tensile strength and modulus of elasticity of tooth structure and several restorative materials. *J Am Dent Assoc* 64:378-387.
- Christensen RM (1990). A critical evaluation for a class of micro-mechanics models. *J Mechan Physics Solids* 38:379-404.
- Cooper WE, Smith DC (1968). Determination of the shear strength of enamel and dentine (abstract). *J Dent Res* 47:997.
- Craig RG, Peyton FA (1958). Elastic and mechanical properties of human dentin. *J Dent Res* 37:710-718.
- Doerner MF, Nix WD (1986). A method for interpreting the data from depth-sensing indentation instruments. *J Mater Res* 1:601-609.
- El Mowafy OM, Watts DC (1986). Fracture toughness of human dentin. *J Dent Res* 65:677-681.
- Featherstone JD, ten Cate JM, Shariati M, Arends J (1983). Comparison of artificial caries-like lesions by quantitative microradiography and microhardness profiles. *Caries Res* 17:385-391.
- Feng G, Ngan AHW (2002). Effects of creep and thermal drift on modulus measurement using depth-sensing indentation. *J Mater Res* 17:660-668.
- Ferry JD (1970). Viscoelastic properties of polymers. New York: John Wiley & Sons, pp. 60-71.
- Gilmore RS, Pollack RP, Katz JL (1969). Elastic properties of bovine dentine and enamel. *Arch Oral Biol* 15:787-796.
- Goodis HE, Marshall GW Jr, White JM, Gee L, Hornberger B, Marshall SJ (1993). Storage effects on dentin permeability and shear bond strengths. *Dent Mater* 9:79-84.
- Gustafson MB, Martin RB, Gibson V, Storms DH, Stover SM, Gibeling J, et al. (1996). Calcium buffering is required to maintain bone stiffness in saline solution. *J Biomechan* 29:1191-1194.
- Gwinnett AJ (1994). A new method to test the cohesive strength of dentin. *Quintessence Int* 25:215-218.
- Habelitz S, Marshall GW, Balooch M, Marshall SJ (2002a). Nanoindentation and the storage of teeth. *J Biomechan* 35:995-998.
- Habelitz S, Balooch M, Marshall SJ, Balooch G, Marshall GW (2002b). In-situ atomic force microscopy of partially demineralized human dentin collagen fibrils. *J Struct Biol* 138:227-236.
- Hashin Z (1983). Analysis of composite materials—a survey. *J Appl Mechan* 50:481-503.
- Huo B, Zheng QS, Zhang Q, Wang JD (2000). Effect of dentin tubules to the mechanical properties of dentin. Part II: Experimental study. *Acta Mechan Sinica* 16:75-82.
- Imbeni V, Nalla RK, Bosi C, Kinney JH, Ritchie RO (2002). On the in vitro fracture toughness of human dentin. *J Biomed Mater Res* (in press).
- Jones RM (1975). Mechanics of composite materials. Washington, DC: Scripta Book Company.
- Jones SJ, Boyde A (1984). Ultrastructure of dentin and dentinogenesis. In: Dentin and dentinogenesis. Linde J, editor. Boca Raton: CRC Press, pp. 81-134.
- Jung HK, Cheong YM, Ryu HJ, Hong SH (1999). Analysis of anisotropy in elastic constants of SiCp/2124 Al metal matrix composites. *Scripta Materialia* 41:1261-1267.
- Katz JL (1971). Hard tissue as a composite material—1. Bounds on elastic behavior. *J Biomechan* 4:455-473.
- Katz JL, Ukraincik K (1971). On the anisotropic elastic properties of hydroxyapatite. *J Biomechan* 4:221-227.
- Kinney JH, Balooch M, Marshall GW, Marshall SJ (1993). Atomic-force microscopic study of dimensional changes in human dentine during drying. *Arch Oral Biol* 38:1003-1007.
- Kinney JH, Balooch M, Marshall SJ, Marshall GW Jr, Weihs TP (1996). Hardness and Young's modulus of human peritubular and intertubular dentine. *Arch Oral Biol* 41:9-13.
- Kinney JH, Balooch M, Marshall GW, Marshall SJ (1999). A micro-mechanics model of the elastic properties of human dentine. *Arch Oral Biol* 44:813-22.
- Kinney JH, Oliveira J, Haupt DL, Marshall GW, Marshall SJ (2001a). The spatial arrangement of tubules in human dentin. *J Mater Sci: Mater Med* 12:743-751.
- Kinney JH, Pople JA, Marshall GW, Marshall SJ (2001b). Collagen orientation and crystallite size in human dentin: a small angle x-ray scattering study. *Calcif Tissue Int* 69:31-37.
- Kinney JH, Gladden J, Marshall GW, Marshall SJ, So JH, Maynard

- JD (2002). Resonant ultrasound spectroscopy measurements of the second order elastic constants in human dentin. *J Biomechan* (in press).
- Kishen A, Ramamurthy U, Asundi A (2000). Experimental studies on the nature of property gradients in the human dentine. *J Biomed Mater Res* 51:650-659.
- Knoop F, Peters G, Emerson WB (1939). A sensitive pyramidal-diamond tool for indentation measurements. *J Res Natl Bur Stds* 23:39-61.
- Korostoff E, Pollack SR, Duncanson MG (1975). Viscoelastic properties of human dentin. *J Biomed Mater Res* 9:661-674.
- Lakes RS, Katz JL (1979). Viscoelastic properties of wet cortical bone: 1. Torsional and biaxial studies. *J Biomechan* 12:657-678.
- Lees S, Rollins FR (1972). Anisotropy in hard dental tissues. *J Biomechan* 5:557-566.
- Lehman ML (1967). Tensile strength of human dentin. *J Dent Res* 46:197-201.
- Lertchirakarn V, Palamara JEA, Messer HH (2001). Anisotropy of tensile strength of root dentin. *J Dent Res* 80:453-456.
- Love AEH (1960). Mathematical theory of elasticity. New York: Dover Press.
- Marshall GW, Marshall SJ, Kinney JH, Balooch M (1997). The dentin substrate: structure and properties related to bonding. *J Dentist* 25:441-458.
- Marshall GW, Yucel N, Balooch M, Kinney JH, Habelitz S, Marshall SJ (2001). Sodium hypochlorite alterations of dentin and dentin collagen. *Surface Sci* 491:444-455.
- Maynard J (1996). Resonant ultrasound spectroscopy. *Physics Today* 49:26-31.
- Migliori A, Sarrao JL, Visscher WM, Bell TM, Lei M, Fisk Z, et al. (1993). Resonant ultrasound spectroscopic techniques for measurement of the elastic moduli of solids. *Physica B* 183:1-24.
- Morgan EF, Yetkinler DN, Constantz BR, Dauskardt RH (1997). Mechanical properties of carbonated apatite bone mineral substitute: strength, fracture and fatigue behaviour. *J Mater Sci: Mater Med* 8:559-570.
- Nalla RK, Imbeni V, Kinney JH, Staninec M, Marshall SJ, Ritchie RO (2002). On the in vitro fatigue behavior of human dentin with implications for life prediction. *J Biomed Mater Res* (in press).
- Nye JF (1972). Physical properties of crystals: their representation by tensors and matrices. Oxford: Oxford University Press.
- Ogawa K, Yamashita Y, Ichijo T, Fusayama T (1983). The ultrastructure and hardness of the transparent layer of human carious dentin. *J Dent Res* 62:7-10.
- Oliver WC, Pharr GM (1992). An improved technique for determining hardness and elastic modulus using load and displacement sensing indentation experiments. *J Mater Res* 7:1564-1583.
- Palamara JE, Wilson PR, Thomas CD, Messer HH (2000). A new imaging technique for measuring the surface strains applied to dentine. *J Dentist* 28:141-146.
- Pashley DA (1989). Dentin: a dynamic substrate—a review. *Scanning Microsc* 3:161-176.
- Pashley D (2001). Private communication.
- Pashley DA, Parham P (1985). The relationship between dentin microhardness and tubule density. *Endod Dent Traumatol* 1:176-179.
- Peyton FA, Mahler DB, Hershenov B (1952). Physical properties of dentin. *J Dent Res* 31:336-370.
- Pidaparti RM, Chandran A, Takano Y, Turner CH (1996). Bone mineral lies mainly outside collagen fibrils: predictions of a composite model for osteonal bone. *J Biomechan* 29:909-916.
- Rasmussen ST (1984). Fracture properties of human teeth in proximity to the dentinoenamel junction. *J Dent Res* 63:1279-1283.
- Rasmussen ST, Patchin RE (1984). Fracture properties of human enamel and dentin in an aqueous environment. *J Dent Res* 63:1362-1368.
- Rasmussen ST, Patchin RE, Scott DB, Heuer AH (1976). Fracture properties of human enamel and dentin. *J Dent Res* 55:154-164.
- Renson CE, Braden M (1975). Experimental determination of the rigidity modulus, Poisson's ratio and elastic limit in shear of human dentine. *Arch Oral Biol* 20:43-47.
- Rho JY, Zioupos P, Currey JD, Pharr GM (1999). Variations in the individual thick lamellar properties within osteons by nanoindentation. *Bone* 25:295-300.
- Ritchie RO (1999). Mechanisms of fatigue-crack propagation in ductile and brittle solids. *Int J Fracture* 100:55-83.
- Roydhouse RH (1970). Punch shear tests for dental purposes. *J Dent Res* 49:131-136.
- Sano H, Ciucchi B, Matthews WG, Pashley DH (1994). Tensile properties of mineralized and demineralized human and bovine dentin. *J Dent Res* 73:1205-1211.
- Sasaki N, Nakayama Y, Yoshikawa M, Enyo A (1993). Stress relaxation function of bone and bone collagen. *J Biomechan* 26:1369-1376.
- Stanford JW, Wiegel KV, Paffenbarger GC, Sweeney WT (1960). Compressive properties of hard tooth tissues and some restorative materials. *J Am Dent Assoc* 60:746-756.
- Staninec M, Marshall GW, Hilton JF, Pashley D, Gansky SA, Marshall SJ, et al. (2002). Ultimate strength of dentin: evidence for a damage mechanics approach to dentin failure. *J Biomed Mater Res* 63:342-345.
- Tengrove HG, Carter GM, Hood JA (1995). Stress relaxation properties of human dentin. *Dent Mater* 11:305-310.
- Tonami K, Takahashi H (1997). Effects of aging on tensile fatigue strength of bovine dentin. *Dent Mater J* 16:156-169.
- van Meerbeek B, Willems G, Celis JP, Roos JR, Braem M, Lambrechts P, et al. (1993). Assessment by nano-indentation of the hardness and elasticity of the resin-dentin bonding area. *J Dent Res* 72:1434-1442.
- Vlassak JJ, Nix WD (1994). Measuring the elastic properties of anisotropic materials by means of indentation experiments. *J Mech Phys Solids* 42:1223-1245.
- Wang RZ, Weiner S (1998a). Human root dentin: structural anisotropy and Vickers microhardness isotropy. *Connect Tissue Res* 39:269-279.
- Wang RZ, Weiner S (1998b). Strain-structure relations in human teeth using Moiré fringes. *J Biomechan* 31:135-141.
- Watanabe LG, Marshall GW, Marshall SJ (1996). Dentin shear strength: effects of tubule orientation and intratooth location. *Dent Mater* 12:109-115.
- Waters NE (1980). Some mechanical and physical properties of teeth. *Symp Soc Exp Biol* 34:99-135.
- Zioupos P, Currey JD, Casinos A (2001). Tensile fatigue in bone: are cycles, or time to failure, or both important? *J Theoret Biol* 210:389-399.